# PREDICTION OF ASPHALT MIXTURE COMPACTABILITY FROM MIXTURE, ASPHALT, AND AGGREGATE PROPERTIES

A Thesis

by

ANDREW JAMES MURAS

Submitted to the Office of Graduate Studies of
Texas A&M University
in partial fulfillment of the requirements for the degree of

MASTER OF SCIENCE

May 2010

Major Subject: Civil Engineering

# PREDICTION OF ASPHALT MIXTURE COMPACTABILITY FROM MIXTURE, ASPHALT, AND AGGREGATE PROPERTIES

A Thesis

by

ANDREW JAMES MURAS

Submitted to the Office of Graduate Studies of
Texas A&M University
in partial fulfillment of the requirements for the degree of

MASTER OF SCIENCE

Approved by:

| | |
|---|---|
| Co-Chairs of Committee, | Eyad Masad |
| | Amy Martin |
| Committee Member, | Charles Glover |
| Head of Department, | John Niedzwecki |

May 2010

Major Subject: Civil Engineering

# ABSTRACT

Prediction of Asphalt Mixture Compactability from Mixture, Asphalt, and Aggregate Properties**.** (May 2010)

Andrew James Muras, B.S., Texas A&M University

Co-Chairs of Advisory Committee: Dr. Eyad Masad
Dr. Amy Martin

The underlying purpose of any pavement is to provide a safe, smooth and reliable surface for the intended users. In the case of hot mix asphalt (HMA) pavements, this includes producing a surface that is resistant to the principal HMA distress types: permanent deformation (or rutting) and fatigue damage (or cracking). To protect better against these distress types, there have recently been changes in HMA mixture design practice. These changes have had the positive effect of producing more damage resistant mixtures but have also had the effect of producing mixtures that require more compaction effort to obtain required densities. It is important to understand what properties of an HMA mixture contribute to their compactability. This study presents analysis of the correlation between HMA mixture properties and laboratory compaction parameters for the purpose of predicting compactability.

Mixture property data were measured for a variety of mixtures; these mixtures were compacted in the laboratory and compaction parameters were collected. A statistical analysis was implemented to correlate the mixture data to the compaction data for the purpose of predicting compactability. The resulting model performs well at

predicting compactability for mixtures that are similar to the ones used to make the model, and it reveals some mixture properties that influence compaction. The analysis showed that the binder content in an HMA mixture and the slope of the aggregate gradation curve are important in determining the compactability of a mixture.

# TABLE OF CONTENTS

Page

Page

# LIST OF FIGURES

Page

Page

# LIST OF TABLES

Page

# CHAPTER I

# INTRODUCTION

Since the start of use of hot mix asphalt (HMA) as a pavement material in the early 1800s, the practice of roadway design has changed much. There have been numerous methodologies used for HMA mixture design. Each design method was intended to provide better results in terms of resistance to the common forms of pavement damage and longer life span. The earlier methods for determining appropriate proportions of asphalt and aggregate were based highly on trial and error and personal experience. As time went on, these methods were replaced by empirically based guidelines for establishing appropriate mixture volumetrics. These guidelines were intended to assist the engineer in developing mixtures that were resistant to both forms of load induced damage: fatigue damage (cracking) and permanent deformation (rutting).

In the 1990s, engineers began to better realize the impact of aggregate size and gradation characteristics on the performance of a mixture. It was determined that aggregates that were angular and rough had better rutting performance than round and smooth aggregates. This relationship has been demonstrated for both coarse and fine aggregates (Huang 2009, and Bennert 2006).

Recent changes in HMA mixture design practices were successful in helping to

---

This thesis follows the style and format of Journal of Materials in Civil Engineering (ASCE).

produce pavements that are resistant to the common distress types but have had the unintended effect of creating some mixtures that are difficult to compact to required densities in the field. This compaction difficulty can lead to pavement performance problems if the required densities are not achieved. There is not yet a reliable method for predicting if a mixture will experience field compaction difficulty. The following sections will describe the background on the topic studied in this thesis, the main problem, and the research tasks.

## BACKGROUND

There have been few studies on methods for predicting mixture compactability. A recent study has focused on relating laboratory measured characteristics of Hot Mix Asphalt (HMA) to field compactability (Leiva 2008). The study indicated a significant correlation between some laboratory and mixture properties and field compaction effort.

Other work on the subject has dealt with more specific topics. One paper investigated how well different laboratory compactors simulated field compaction (Khan 1998). Others dealt with how specific mixture properties like fine aggregate angularity (FAA) and temperature affected laboratory compaction (Stakston 2002 and Lee 2008). These studies found that mixtures with higher FAA required greater compactive effort, and mixtures compacted at lower temperatures resulted in greater air void contents.

In every study relating to HMA compaction, there must be some measure to quantify laboratory compaction or the compactability of mixtures. Often this can be

done using simple measures like the air void content after a set number of gyrations in a compactor; sometimes more complicated indexes are used. Frequently the number of gyrations required to achieve a specific density or the maximum density is used.

Delgadillo (2008) used the percent theoretical maximum specific gravity ($\%G_{mm}$) at the first gyration, the design number of gyrations, and the maximum number of gyrations to measure compaction. Stakston (2002) used three similar $\%G_{mm}$ values to quantify compaction but also used two compaction indexes, which are the compaction densification index (CDI) and compaction force index (CFI). The (CDI) is calculated by integrating the area under the densification curve from the first gyration to $92\%G_{mm}$. The (CFI) is calcualated by integrating the area under the resistive work curve measured using a gyratory load plate assembly.

In the study by Leiva(2008), the compaction parameters used were density at the first gyration, compaction slope, number of gyrations to achieve 92% theoretical maximum specific gravity ($G_{mm}$), compaction energy index (CEI), and the number of gyrations to reach the locking point. Here, the compaction slope is the slope of a line from the beginning of compaction to the end, the CEI is the area under a compaction curve from the eighth gyration to a certain density, and the locking point is the first gyration where no increase in density is measured. That study found that CEI, N at 92% $G_{mm}$, compaction slope, and locking point were good measures of laboratory compactability.

## PROBLEM STATEMENT

While there is not a great deal of evidence that HMA mixture compaction issues have become a serious problem in the asphalt industry, there is a desire to estimate the ability to compact a mixture prior to the start of pavement construction. The purpose of this study is to develop a correlation between HMA mixture properties and compaction parameters for the purpose of predicting compatibility in the laboratory. This correlation could be useful to determine the level of compaction effort that is needed in the field in order to achieve the desired densities. In addition, it can be used to determine the possible effects of manipulating mixture properties to facilitate compaction.

In order to produce this correlation, many different mixtures and mixture types were prepared. For each mixture, certain properties describing the asphalt binder, gradation, and aggregates were measured. Hot mix asphalt (HMA) specimens were compacted for each mixture, and compaction parameters for each specimen were recorded. A correlation was found between the mixture properties and the compaction parameters.

## RESEARCH TASKS

This section will outline and summarize the research tasks taken in t his study. These tasks are as follows.

- Conduct literature review on asphalt compaction.

- Collect data of HMA mixture characteristics and compaction.
- Carry out statistical analysis of the relationship between mixture characteristics and compaction data using Number of Factors, Neural Net, and Stepwise Regression methods.

# CHAPTER II

# EXPERIMENTAL DESIGN AND RESULTS

This chapter describes the HMA mixtures used for the study, the mixture properties that were measured, and how these properties were measured or calculated. The first phase of this project involved the collection, compaction, and testing of many different HMA mixtures. The laboratory compaction and testing was performed at the McNew Materials Testing Laboratory at Texas Transportation Institute (TTI). The different HMA mixture types included in the study were crack attenuating mixtures (CAM), dense graded mixtures (B, C, and D), Stone Matrix Asphalt (SMA), and Porous Friction Course (PFC). These are all Texas Department of Transportation (TxDOT) mixture design types (TxDOT 2008). These mixture types differ mainly in their gradations, maximum aggregate size, and also in the amount of asphalt binder typically used. CAMs are characterized by including fine gradations and large asphalt contents. They are used primarily as an interlayer between an existing pavement and a surface layer. Dense graded mixtures are produced with continuously graded aggregate. Among dense graded mixtures, mixture type B has the largest maximum aggregate size, followed by mixture type C and then mixture type D. SMAs are gap-graded, meaning they contain large amounts of coarse and fine aggregate but very little intermediate aggregate. They are typified by stone-on-stone contact and often contain fibers or modified binders. PFC mixtures are open-graded, meaning they are produced with mainly uniform-sized aggregate. They are known for producing less road noise than

other mixtures and for their ability to drain water from the pavement surface. The test mixture pool was intended to include several examples of each mixture type to ensure a diverse set. Table 1 shows the number of mixtures of each type that were used.

**Table 1 Types and Number of Mixtures Used in This Study**

| Mixture Type | Number of Mixture |
|---|---|
| **B** | 2 |
| **C** | 6 |
| **D** | 3 |
| **CAM** | 7 |
| **SMA** | 3 |
| **PFC** | 1 |

The following mixture characteristics and properties of mixture constituents were measured:

- binder content,
- binder viscosity,
- gradation parameter $\lambda$, $k$,
- aggregate angularity,
- aggregate texture,
- aggregate sphericity,

## BINDER CONTENT AND VISCOSITY

Binder content is the percent mass of asphalt binder per total mass of the mixture. This value generally can range from as low as 4% to as high as 9% depending on the aggregate and mixture type. The binder viscosity is the resistance to flow of the asphalt binder. The rotational viscosity of the binder was measured at the mixture compaction temperature using a Brookfield Rotational Viscometer (AASHTO T316). In this test, a small container of asphalt binder is heated to the compaction temperature. A small steel cylinder is immersed into the binder and rotated at a constant rate. The machine measures the torque required to rotate the spindle at that rate. Using this information along with some attributes of the spindle, the machine calculates a rotational viscosity for the binder. Figure 1 shows the Brookfield Rotational Viscometer along with a small heater to warm the binder and the controlling computer. Table 2 lists the viscosity of the binder used in each mixture along with the binder content and testing temperature. The testing temperature is determined by the PG grade of the binder used in each mixture. The compaction temperature for each binder was chosen for testing in accordance with Texas Department of Transportation guidelines (TxDOT).

**Figure 1. Brookfield Rotational Viscometer**

**Table 2 Asphalt Binder Content and Viscosity**

| Mixture Name, Type | Binder Content % | Binder Viscosity cP | Temperature at measured Viscosity °C |
|---|---|---|---|
| US 87 C | 4.3 | 1167.5 | 149 |
| HW 6 SMA_D | 6.4 | 656.7 | 149 |
| SH 44 B | 4.2 | 777.5 | 149 |
| SH 21 C | 4.7 | 883.4 | 135 |
| Lufkin CAM 7.0% 70-22 | 7 | 890.0 | 135 |
| Lufkin CAM 7.5% 70-22 | 7.5 | 890.0 | 135 |
| Lufkin CAM 8.0% 70-22 | 8 | 890.0 | 135 |
| Lufkin CAM 7.5% 76-22 | 7.5 | 824.8 | 149 |
| Lufkin CAM 8.0% 76-22 | 8 | 824.8 | 149 |
| Lufkin CAM 8.5% 76-22 | 8.5 | 824.8 | 149 |
| Mopac SMA_C | 6.2 | 824.8 | 149 |
| Bryan C | 4.4 | 1238.3 | 121 |
| SS3111_CAM | 7.6 | 824.8 | 149 |
| I-35 Waco SMA_D | 6 | 684.2 | 149 |
| SH 36 D | 4.9 | 1205.0 | 121 |
| US 259 C | 4.3 | 919.2 | 135 |
| 341 C | 4.5 | 1190.8 | 135 |
| 346 SMA | 6 | 824.8 | 149 |
| 342 PFC | 6.7 | 1205.0 | 149 |
| 340 B | 4.6 | 1228.3 | 121 |
| Arash4 C | 4.5 | 730.0 | 149 |
| Arash9 D | 5.3 | 730.0 | 149 |

## AGGREGATE GRADATION

The gradation of an asphalt mixture describes the amount and size of the aggregate particles that make up the mixture. Aggregate gradations are shown graphically by plotting the size of the aggregates versus the percent of total aggregate

weight passing each sieve size. Different mixture types can have dramatically different gradation curves. In order to characterize these differences in gradation, a Weibull distribution curve was fit to each gradation curve using a least squares method as shown by the example in Figure 2. The form of the Weibull distribution used is shown in Equation 1.

$$P = 1 - e^{-\left(\frac{x}{\lambda}\right)^k} \quad \textbf{(1)}$$

In the equation, $x$ is the size in millimeters of each sieve used in the gradation, $P$ is the percent passing each sieve size, and $\lambda$ and $k$ are shape and scale parameters. These two parameters determine the broad shape of the curve. The fit was found using the Solver tool in Microsoft Excel. The difference between the percent passing at each sieve size and the equation predicted percent passing was squared and summed for all the sieve sizes. This summed difference is called the squared error. The Solver manipulates $\lambda$ and $k$ to find the minimum squared error.

Figure 2 shows the aggregate gradation curve for two mixtures, one type C mixture, and a PFC mixture. It also shows the predicted curve resulting from the Weibull distribution fit. The predicted curves mirror the actual curves well. For these two mixtures, the gradation shape parameter $\lambda$ for the C and PFC mixture is 4.74 and 9.76, respectively. The gradation scale parameter $k$ for the C and PFC mixture is 0.85 and 2.83, respectively.

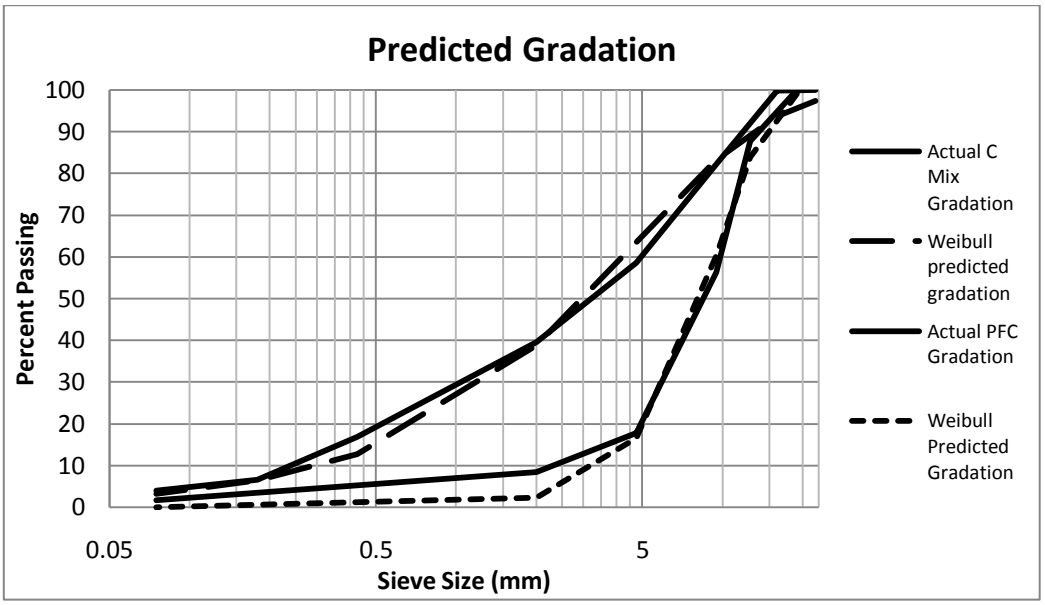


**Figure 2. Examples of Weibull Distribution Fit to Aggregate Gradations**

Prior studies relating mixture gradation to compaction or performance simply described the gradation qualitatively such as fine, coarse, gap, or open graded. The Weibull distribution method uses two numerical values to describe the shape of the gradation curve rather than a just the mixture type. Table 3 shows the gradation parameters for all the mixtures used in the study. The values of $\lambda$ ranged from 3.17 for a CAM mixture to 9.76 for a PFC mixture. In a broad sense, manipulating the values of $\lambda$ has the effect of shifting the gradation curve to the left and right. This shifting of the curve affects the size of the aggregates. Manipulating the value of *k* changes the slope of the curve. This slope distinguishes well graded gradations from gap graded gradations. The *k* parameter ranges from 0.75 for a B mixture to 2.38 for the PFC mixture.

**Table 3 Parameters of Weibull Distribution Function for Various Gradations**

| Mixture Name | Type | Gradation λ | Gradation k |
|---|---|---|---|
| US 87 | C | 4.74 | 0.85 |
| HW 6 | SMA_D | 9.20 | 1.49 |
| SH 44 | B | 5.51 | 0.75 |
| SH 21 | C | 5.47 | 0.85 |
| Lufkin | CAM 7.0% 70-22 | 3.17 | 1.00 |
| Lufkin | CAM 7.5% 70-22 | 3.17 | 1.00 |
| Lufkin | CAM 8.0% 70-22 | 3.17 | 1.00 |
| Lufkin | CAM 7.5% 76-22 | 3.17 | 1.00 |
| Lufkin | CAM 8.0% 76-22 | 3.17 | 1.00 |
| Lufkin | CAM 8.5% 76-22 | 3.17 | 1.00 |
| Mopac | SMA_C | 9.43 | 1.28 |
| Bryan | C | 4.42 | 0.77 |
| SS3111 | CAM | 3.23 | 0.92 |
| I-35 Waco | SMA_D | 8.87 | 1.36 |
| SH 36 | D | 4.34 | 0.92 |
| US 259 | C | 5.97 | 0.83 |
| 341 | C | 4.95 | 0.79 |
| 346 | SMA | 9.14 | 1.50 |
| 342 | PFC | 9.76 | 2.38 |
| 340 | B | 7.06 | 0.86 |
| Arash 4 | C | 5.33 | 0.79 |
| Arash 9 | D | 4.30 | 0.81 |

Figures 3-8 show sample gradation curves for the mixture types used in the study. The original curves are shown by the solid line; the dashed-lines are the curves produced by the Weibull distribution function. In most cases the Weibull fit curve follows the original curve reasonably well.

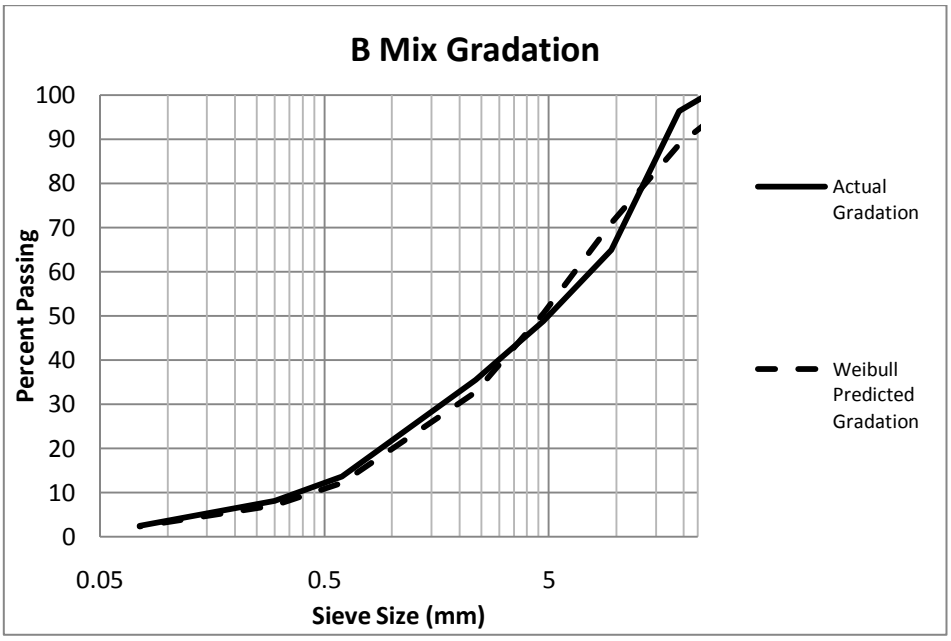


**Figure 3. Sample B Mix Gradation**

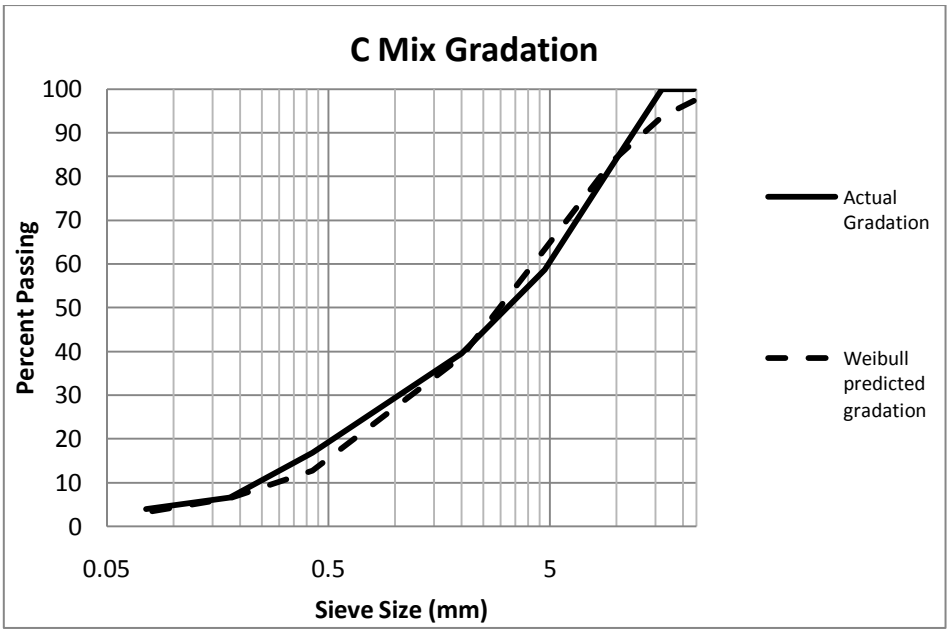


**Figure 4. Sample C Mix Gradation**

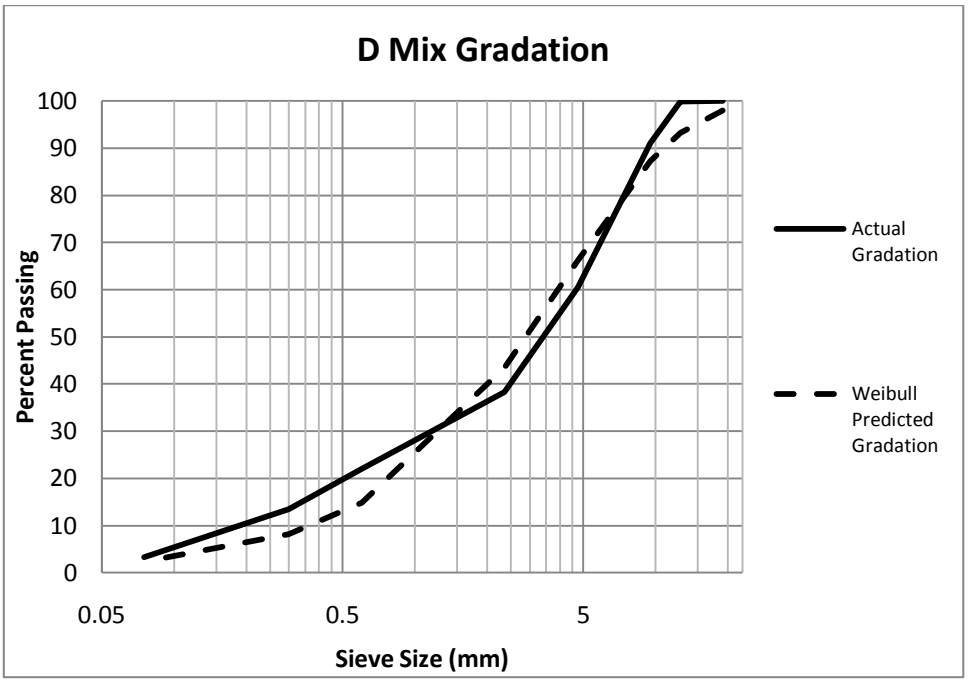


**Figure 5. Sample D Mix Gradation**

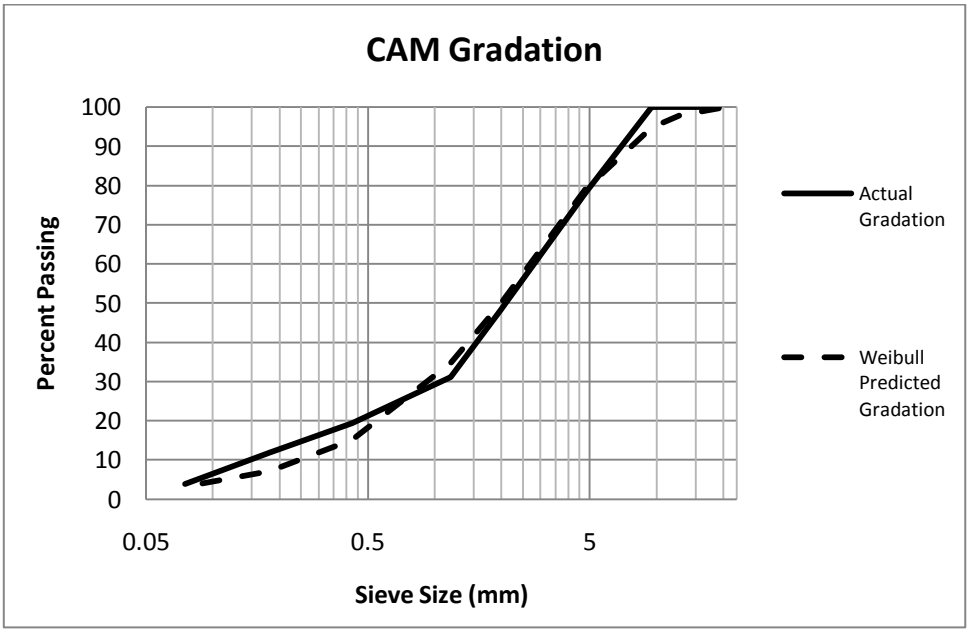


**Figure 6. Sample CAM Mix Gradation**

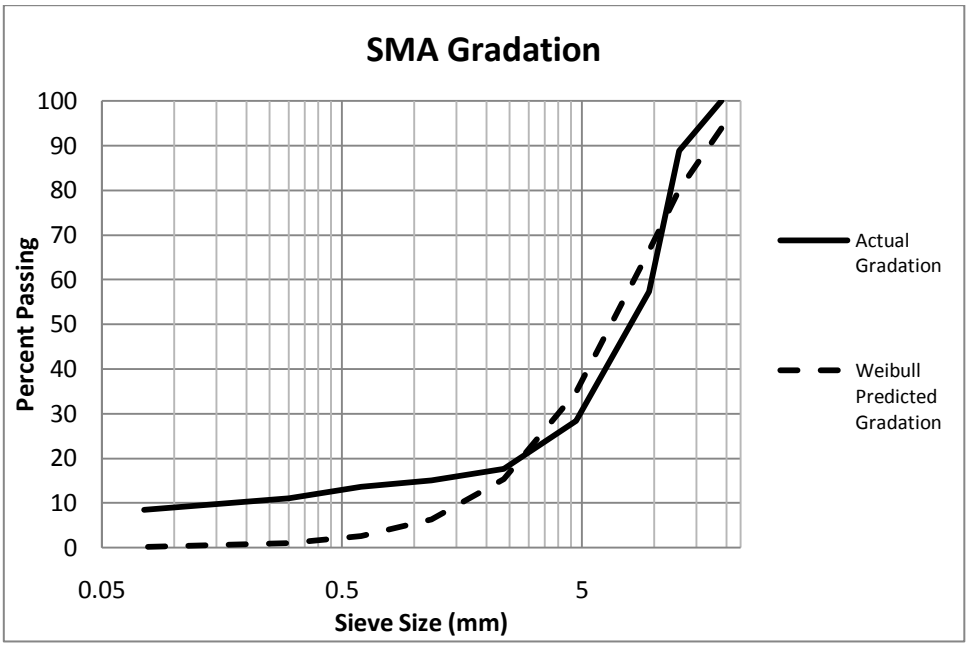


**Figure 7. Sample SMA Mix Gradation**

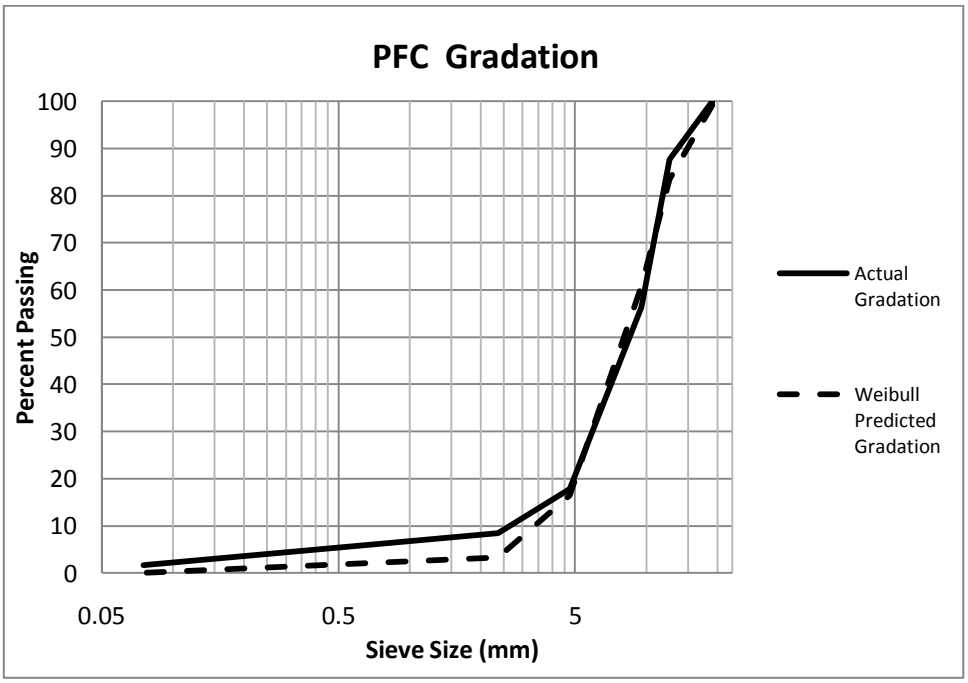


**Figure 8. Sample PFC Mix Gradation**

## AGGREGATE SHAPE CHARACTERISTICS

The Aggregate Imaging System (AIMS) was used to quantify the shape characteristics of aggregates (Fletcher 2003). The AIMS system uses a digital camera to take detailed wider angle photographs of entire aggregates or close up photographs of the surface of aggregates. The system software uses these images to calculate various aggregate shape and texture properties including 2D form, angularity, sphericity, texture, and flat and elongated ratio. For this study, angularity, texture, and sphericity were utilized. Figure 9 shows the AIMS apparatus. It consists of a servo-controlled, illuminated platform that the aggregates are placed on, a digital camera and lights mounted above the platform, electronics, and a controlling computer.

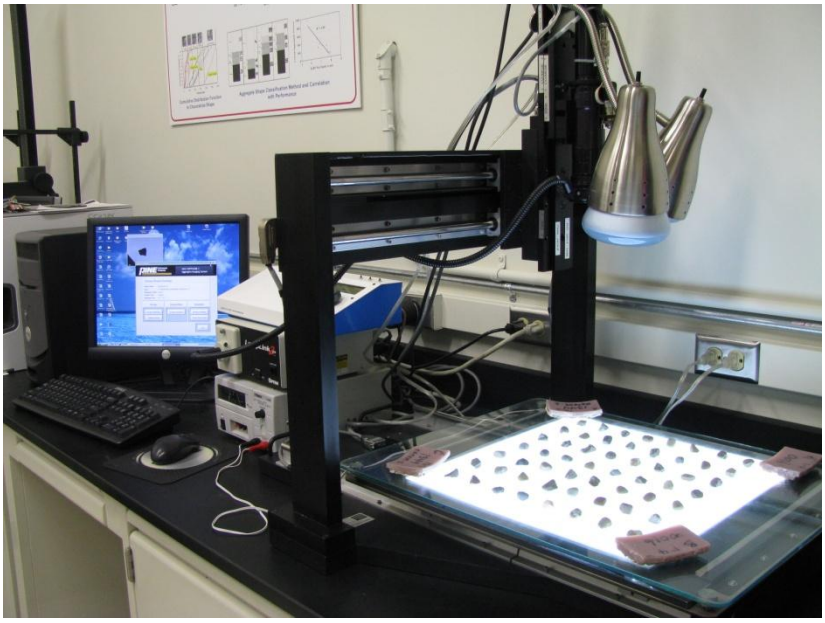

**Figure 9. Aggregate Imaging System (AIMS)**

To calculate angularity, AIMS captures a 2D, black and white digital image of each aggregate particle. The program calculates a numerical angularity index value for each aggregate using the gradient method. The method used to calculate the average in the change in the angles of orientation of the gradient vectors around the edge of the particle outline. Faceted particles will have a higher angularity index than rounded particles since the angles of orientation change more rapidly near sharp corners (Mahmound 2008). Figures 10 and 11 show black and white digital images taken by the AIMS camera of low and high angularity aggregates respectively.

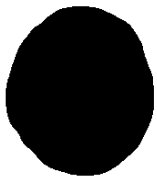

**Figure 10. A Projection of a Low Angularity Aggregate Particle**

**Figure 11. A Projection of a High Angularity Aggregate Particle**

Aggregate texture index values are found by taking a close up grey scale image of the aggregates surface and calculating the texture using wavelet analysis. The AIMS software calculates texture by finding the local variation in the pixel gray-intensity values. A more detailed explanation of this analysis is available in Fletcher (2003). Figures 12 and 13 are digital grey-scale images taken by the AIMS camera of a low and high texture aggregate, respectively.

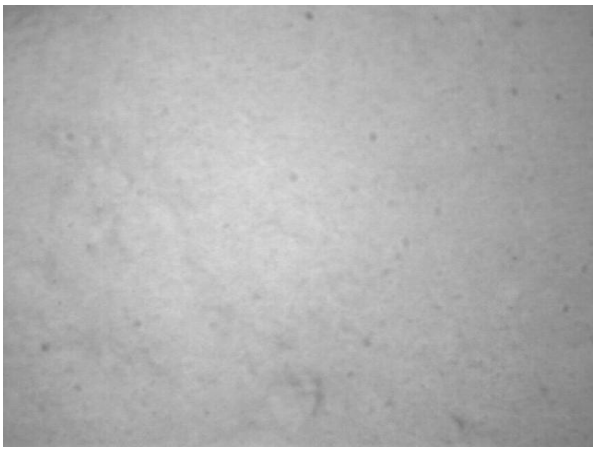

**Figure 12. An Image of the Surface of Low Texture Aggregate**

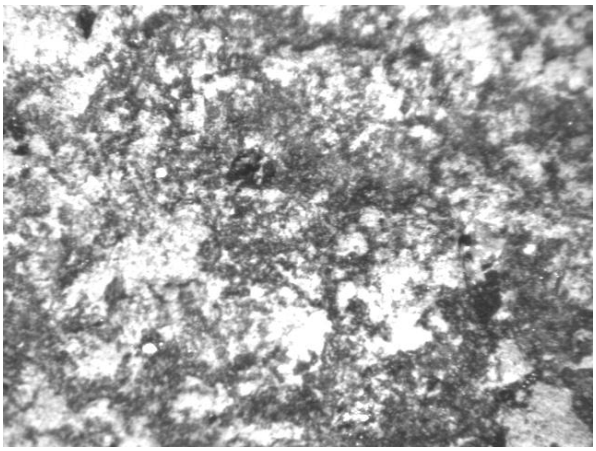

**Figure 13. An Image of the Surface of High Texture Aggregate**

Sphericity is found using length, width, and depth measurements of each aggregate particle. The 2D grey-scale image is used to find the longest and shortest dimensions of the aggregate projection. The autofocus feature on the camera is used to measure the thickness. Equation 2 is used to calculate sphericity. Texture and sphericity

can only be measured for aggregates retained on a 4.75 mm sieve. Aggregates smaller than 4.75 mm are only tested for angularity.

$$Sphericity = \sqrt[3]{\frac{d_S \times d_I}{d_L^2}} \quad (2)$$

Before AIMS testing can begin for aggregates use in an HMA mixture, there are a few steps that must be taken in preparation. The system is designed to scan only one size of aggregate at the same time. Aggregates must be sieved and separated by their sizes. For the study, the sieve sizes used to separate aggregate were 0.75", 0.5", 0.375", 0.25", No.4, No.8, and No.16. This separation must be done for every bin present in the aggregate gradation.

After each bin is sieved into its constituent sizes, the aggregates must be washed and dried before they can be scanned. This removes fine particles from the aggregate surface that could affect the measurements.

Once the aggregates were washed and dried, they were ready for testing. From each bin, one coarse aggregate size, usually 3/8", No. 8, and No. 16 were scanned. During testing, shape characteristics were measured for each aggregate. The computer program compiles all the results for each test and calculates the average and standard deviation values. It also creates plots showing the distribution of characteristic values for each test. Figures 14, 15, and 16 show examples of distribution curves produced by the AIMS system for the shape characteristics used in the study.

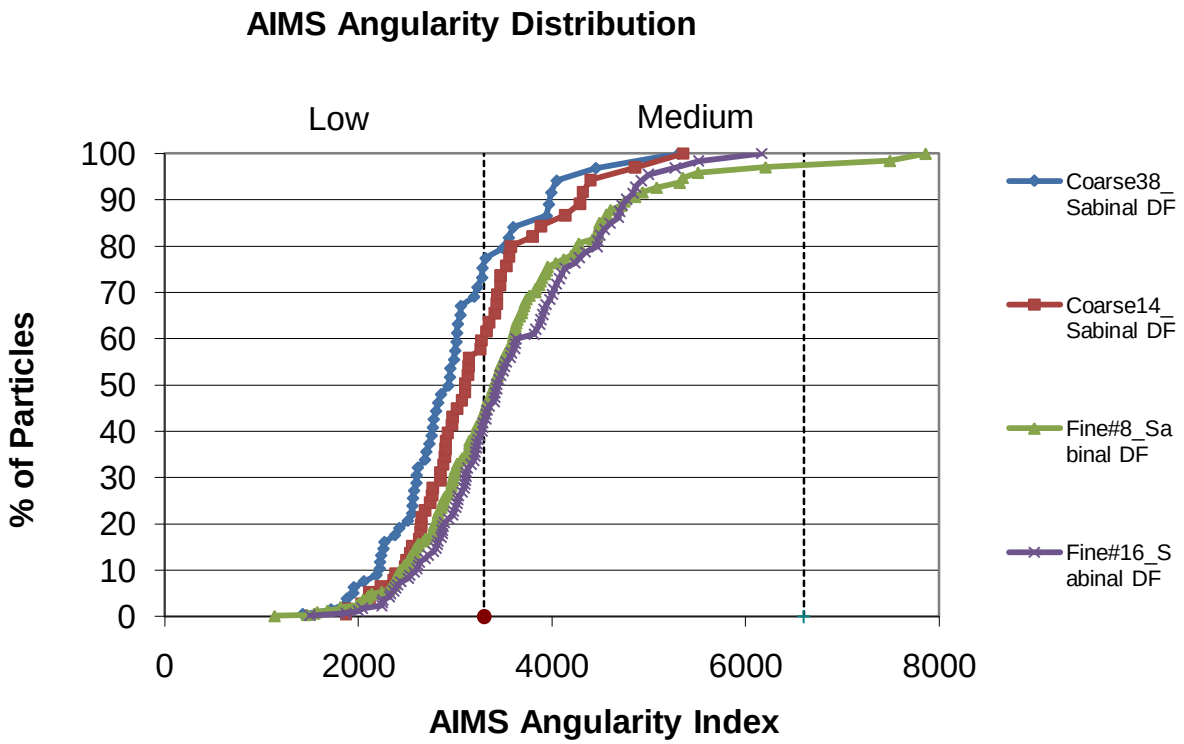


**Figure 14. Example of AIMS Measurements of Angularity Distribution**

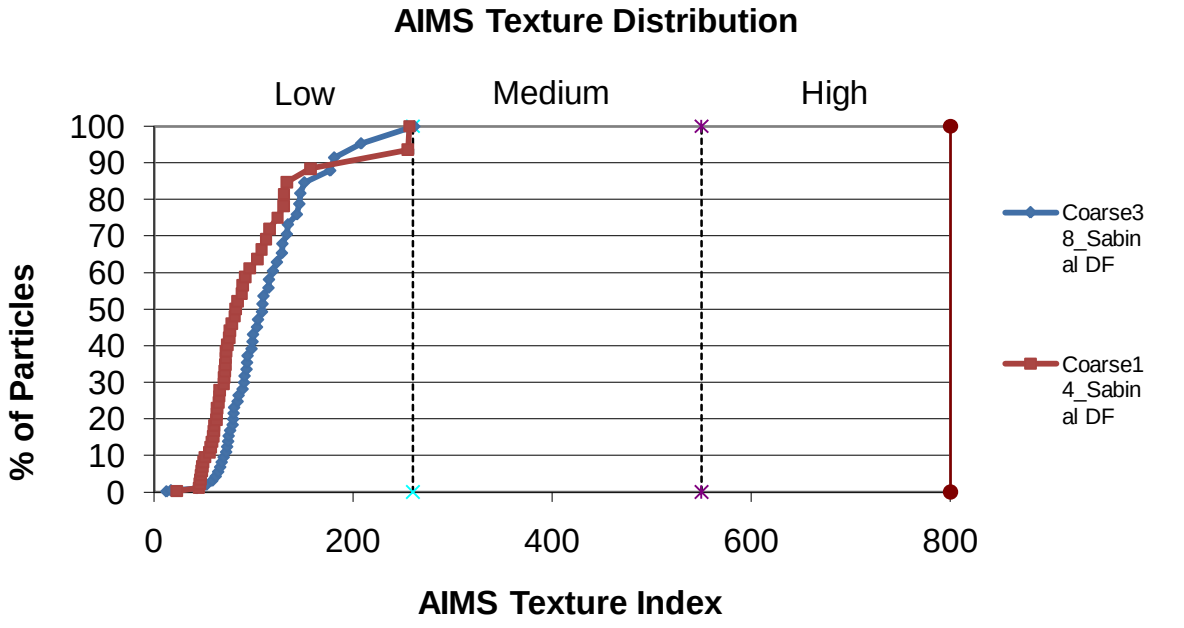


**Figure 15. Example of AIMS Measurements of Texture Distribution**

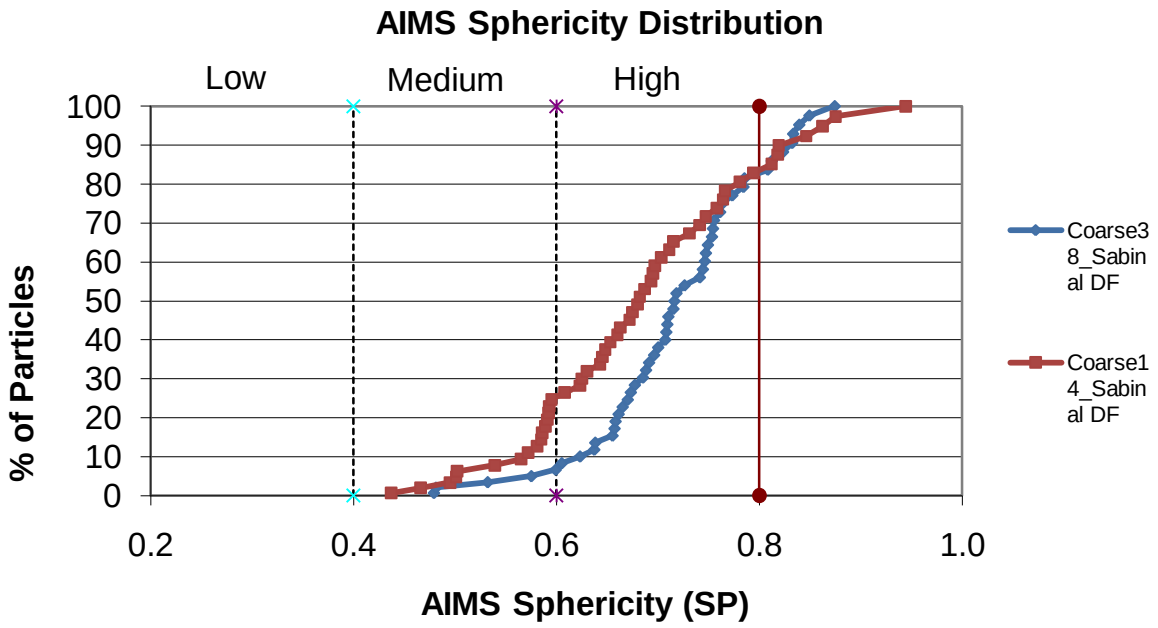


**Figure 16. Examples of AIMS Measurements of Sphericity Distribution**

For the purposes of this study, it is desirable to have just one average value of angularity, texture, and sphericity for each HMA mixture. The AIMS software calculates a weighted average of shape characteristics for each aggregate bin. For angularity and texture measurements, the average is weighted by the surface area of the aggregates. A typical particle volume and mass is calculated assuming a cubical shape with length, width, and height measurements equal to half the smallest passing sieve and the largest retaining sieve for each size. Using this typical particle, the bin gradation, and the shape characteristic values for each size scanned from the bin, the program calculates a weighted average. The program uses the same procedure for sphericity except it weights the average by particle count in the gradation and not surface area.

Using the average shape characteristic values for each bin and the percentages of each bin present in the mixture, a weighted average must again be calculated, this time for the entire mixture. Angularity and texture are again weighted by surface area, and sphericity is weighted by particle count. Table 4 contains the average shape characteristic values for all the aggregate gradations used in the study.

**Table 4 Average Aggregate Shape Characterisitcs**

| Mixture Name, Type | Angularity | Texture | Spherisity |
|---|---|---|---|
| US 87 C | 2981.1 | 160.8 | 0.722 |
| HW 6 SMA_D | 3067.2 | 210.0 | 0.665 |
| SH 44 B | 2818.7 | 177.5 | 0.737 |
| SH 21 C | 2811.9 | 106.0 | 0.708 |
| Lufkin CAM 7.0% 70-22 | 3895.1 | 337.7 | 0.690 |
| Lufkin CAM 7.5% 70-22 | 3895.1 | 337.7 | 0.690 |
| Lufkin CAM 8.0% 70-22 | 3895.1 | 337.7 | 0.690 |
| Lufkin CAM 7.5% 76-22 | 3895.1 | 337.7 | 0.690 |
| Lufkin CAM 8.0% 76-22 | 3895.1 | 337.7 | 0.690 |
| Lufkin CAM 8.5% 76-22 | 3895.1 | 337.7 | 0.690 |
| Mopac SMA_C | 3822.7 | 172.6 | 0.730 |
| Bryan C | 2681.1 | 106.0 | 0.739 |
| SS3111_CAM | 3477.0 | 546.7 | 0.620 |
| I-35 Waco SMA_D | 2848.1 | 375.1 | 0.690 |
| SH 36 D | 3104.1 | 63.7 | 0.675 |
| US 259 C | 3065.3 | 366.8 | 0.760 |
| 341 C | 3523.5 | 96.2 | 0.679 |
| 346 SMA | 2787.4 | 143.1 | 0.657 |
| 342 PFC | 2995.6 | 82.2 | 0.661 |
| 340 B | 2697.7 | 149.0 | 0.748 |
| Arash4 C | 2885.8 | 294.3 | 0.694 |
| Arash9 D | 2801.8 | 283.9 | 0.681 |

## AGGREGATE MIXTURE COMPACTION

After mixture data were collected for each mixture, samples were compacted in the laboratory. Samples were compacted using the Superpave Gyratory Compactor (SGC). Figure 17 shows the SGC used for the study. Compaction using a SGC involves first placing HMA mixture into a heated steel cylindrical mold with a 6-inch diameter. Once placed inside the compactor, a pneumatic ram applies 600kPa pressure on the material and the ram gyrates in a circular pattern at a 1.25 degree angle at a constant rate of 30 revolutions per minute. Material inside the mold loses its air void content as the sample shrinks in height. Dimensions of the compaction test samples were 6 inches in diameter and 2.5 inches in height. This sample size was chosen because most of the specimens were prepared to be tested using the laboratory tests, Hamburg Wheel Tracking test and the Overlay test. Four replicate samples were compacted for each mixture type.


**Figure 17. The Superpave Gyratory Compactor (SGC) Used in This Study**

Once aggregate and asphalt binder were obtained for each mixture, aggregate for four replicate samples was weighed out and prepared for compaction. Appropriate mixing and compaction temperatures guidelines for each type of PG grade binder were followed (TxDOT). A listing of the TxDOT recommended mixing and compaction temperatures is shown in Table 5. Most HMA mixture designs included important

information about the aggregate bin proportions required, binder PG grade and content, and the theoretical maximum specific gravity ($G_{mm}$) of the mixture at the optimum binder content. Samples were compacted to a target air void content of 7% for most mixtures except PFC, which were compacted to 15% air voids. PFCs have a much more open aggregate gradation and cannot be compacted to the same densities as other mixtures. Using the $G_{mm}$, the target air void content, and the sample volume at the required dimensions, the appropriate weight of material for each sample was calculated. The specific SGC compactor used has the ability to terminate compaction once it reaches a specified number of gyrations or when the sample reaches a specified height or air void content. For this study, each compaction was set to end when the sample reached 2.5 inches in height.

**Table 5 HMA Mixing and Compaction Temperatures**

| **HMA Mixing and Compaction Temperatures by Grade** | | |
|---|---|---|
| **PG Grade** | **Mixing Temp, °F** | **Compaction Temp, °F** |
| 64-22 | 290 | 250 |
| 64-28 | 300 | 275 |
| 70-22 | 300 | 275 |
| 70-28 | 325 | 300 |
| 76-16 | 325 | 300 |
| 76-22 | 325 | 300 |

Following compaction of samples for each mixture, some loose material was reserved for laboratory testing of $G_{mm}$ using the pycnometer method (ASTM D 2041). Results of the $G_{mm}$ test were compared to the posted value on the mixture design report that accompanied each mixture design. If there was a significant discrepancy in the two values, it was noted and the laboratory measured value was used for all later calculations.

Once each laboratory molded sample had sufficiently cooled, its bulk specific gravity ($G_{mb}$) was measured using the CoreLok machine (AASHTO PT 69). Figure 18 shows the CoreLok tester. This testing method involves sealing a plastic bag around the sample while it is under a vacuum so that the surface air voids of the sample are filled in. This ensures that the volume contained inside the bag is occupied only by the sample and no air. This sealed sample is then submerged and weighed under water. Figure 19 shows a laboratory compacted sample sealed inside an air tight plastic bag.


**Figure 18. The CoreLok Tester Used to Measure Specimen Specific Gravity**

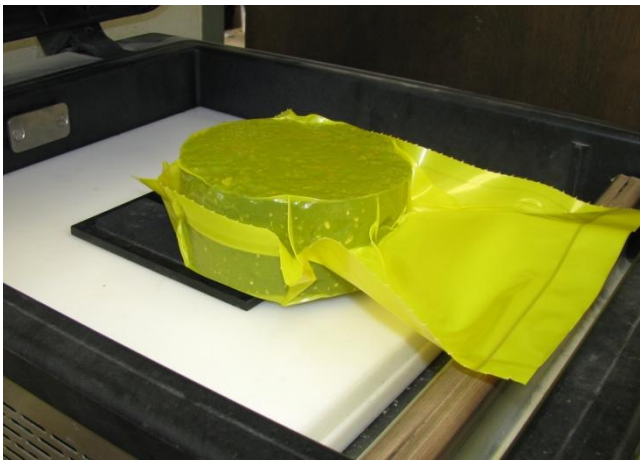

**Figure 19. CoreLok Sealed Sample**

These two laboratory tests were conducted because with their results ($G_{mm}$, $G_{mb}$) the density or air void content (%AV) of the samples could easily be calculated. The samples were compacted to a specific air void content, but it is important to measure the

actual content in the samples. HMA laboratory samples have two types of air voids, internal voids and surface voids. For most purposes, data on only the internal voids is desired. When samples are molded to a specific air void content based on their $G_{mm}$ value and dimensions (when compaction is set to terminate when a sample reaches a specific AV), this includes both internal and surface voids. The CoreLok test is designed to measure only the internal voids. This is done by assuming that under vacuum, the plastic bag conforms to the surface of the sample, filling in most surface voids.

The specific SGC compactor used for the study has the ability to save a file for each compaction completed. Each file contains general data about the test including date, time, sample diameter, gyration rate, vertical stress, gyration angle, weight of material, and $G_{mm}$. The files also contain information about each gyration in a compaction test including gyration number, sample height, and shear stress. The height per gyration data is most valuable because it can be used to construct a compaction curve for each sample. Figure 20 contains a compaction curve showing sample height versus gyration number.

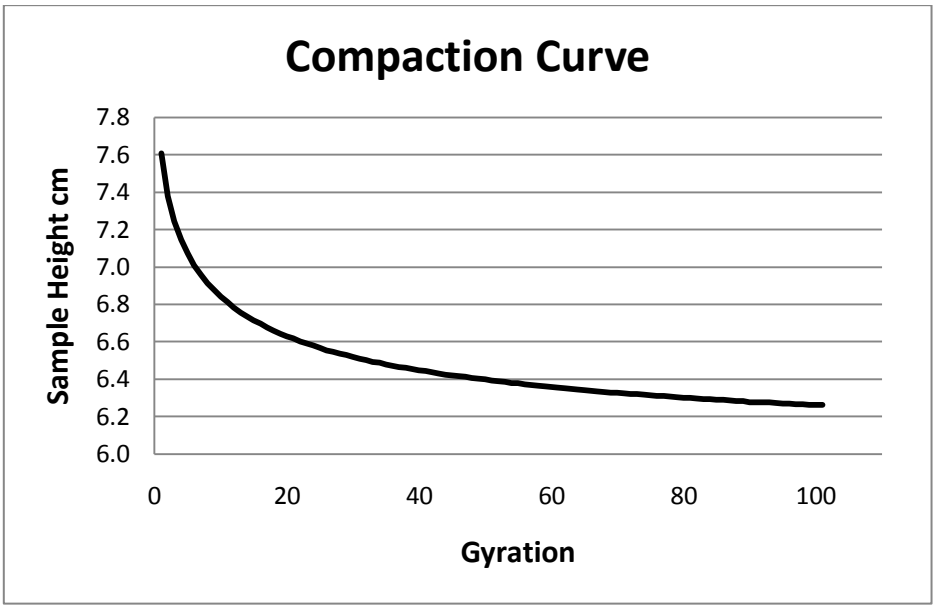


**Figure 20. An Example of Compaction Curve Showing Sample Height Change as a Function of Number of Gyrations**

With the height versus gyration data, as well as the weight, radius, and $G_{mm}$ for each sample the air voids versus gyration curves can be calculated volumetrically using Equation 3.

$$AV = 100\left(1 - \frac{\frac{weight}{\pi * r^2 * height}}{G_{mm}}\right) \quad (3)$$

Equation 3 accurately calculates the air voids content at each gyration volumetrically, but one drawback is this method includes air voids on the surface of the samples. As stated before, for most purposes the amount of internal air voids is desired. To correct this problem, the CoreLok measured air void content of each sample and the

volumetrically measured content are used to calculate a correction factor. This correction factor is used to adjust the %AV at each gyration in the curve. A summary of this calculation is available in Appendix A. An example of a corrected %AV versus gyration compaction curve is shown in Figure 21.

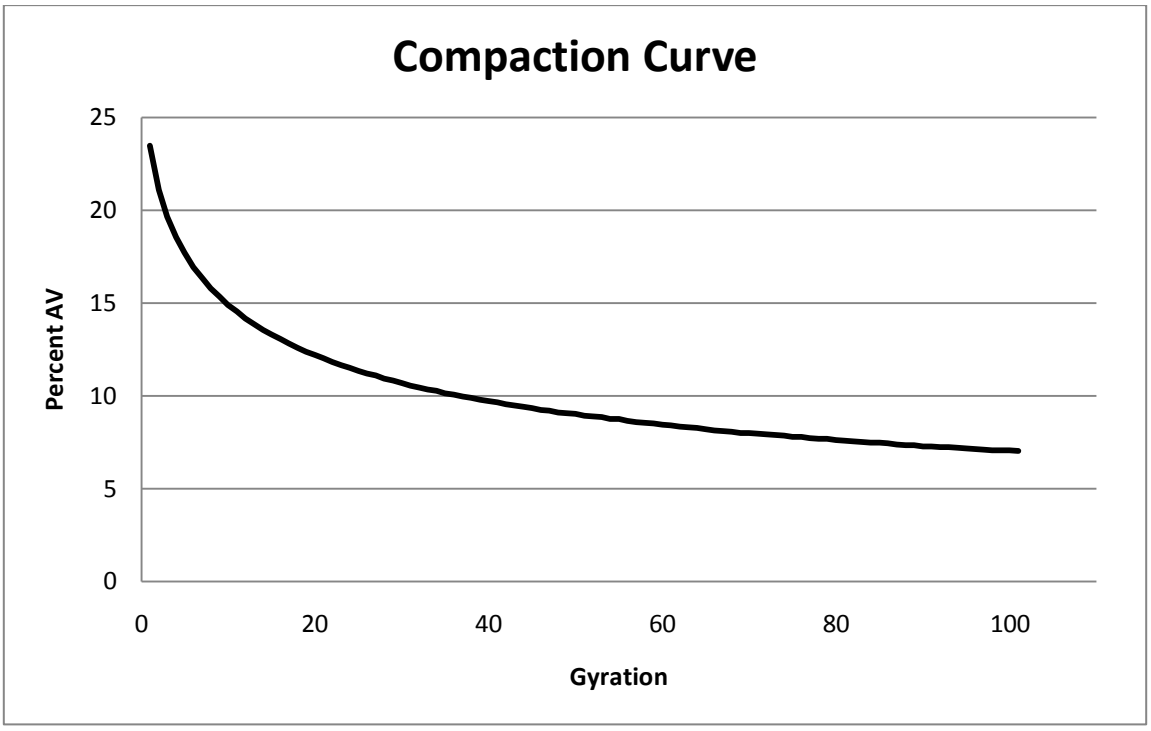


**Figure 21. An Example of Corrected Air Void Versus Number of Gyrations Curve**

## COMPACTION PARAMETERS

Following collection of HMA mixture property data and compaction of test samples, the next step was to extract compaction parameters from the compaction curves of each sample. It was believed that different mixture properties might affect different

parts of the compaction curve. For instance, asphalt binder content might have a greater influence on the slope of the compaction curve early in the compaction, while slopes near the end of compaction might be greater influenced by aggregate angularity. It is important to understand how different properties of HMA mixtures affect different parts of the compaction curve. There was also an ongoing study by another TTI researcher that sought to correlate laboratory compaction parameters to field compaction. This complimentary study required five laboratory compaction parameters. To characterize these different parts of a normalized compaction curve described subsequently, the following seven compaction parameters were extracted from the data:

- $a$ Slope of normalized compaction curve,
- $c$ y-axis intercept of normalized compaction curve,
- $\%AV\ N_{ini}$ Sample %AV after first gyration,
- $m_1$ Linear slope of first five gyrations,
- $m_2$ Linear slope of gyrations 96 to 100,
- $\alpha$ Gyration at intercept of $m_1$ and $m_2$ lines,
- $\Delta\ Slope$ Difference between $m_1$ and $m_2$,

In identifying the various compaction parameters, one of the first steps was to fit a trendline to the compaction curve of each sample. This was first done by plotting the %AV versus number of gyrations in Excel and fitting a trendline to the curve. It was found that a logarithmic equation with a slope and y-axis intercept fits the curves best.

Figure 22 shows two air void compaction curves from different mixtures; one is a type C mixture and the other is an SMA mixture. The trendline and corresponding equation and $R^2$ value are shown for both curves. As evident by the high $R^2$, a logarithmic equation fits the data very well.

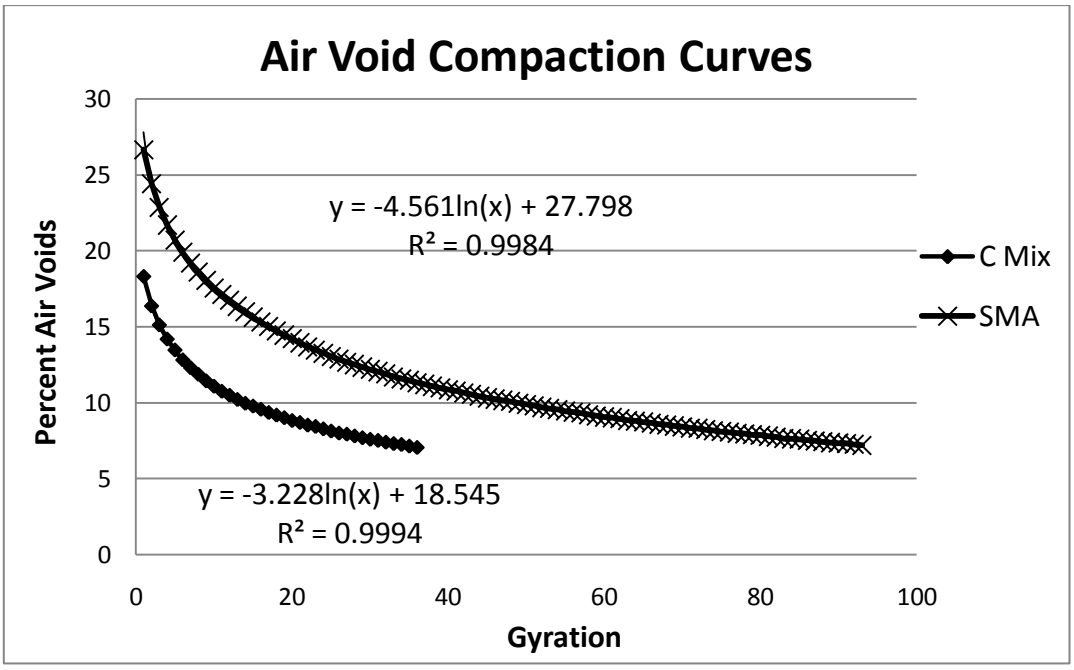


**Figure 22. Air Void Compaction Curves**

In addition to the slope and intercept, additional parameters related to the amount of compaction at a specific gyration number or a specific %AV were considered. This representation of the compaction curves works well for describing different curves when each compaction has the same final %AV. In that case, a possible parameter could be the gyration at which the sample reaches its target %AV. Another parameter could be the percent compaction at a set number of gyrations. Since all the curves were adjusted

by the CoreLok measured %AV, and mixture types like PFC (which is designed to a higher %AV range) were included, this type of parameter was no longer usable. The final %AV of different mixtures ranged from 5% to 15%. Achieving 15%AV, for example, in two mixtures with different final %AV corresponds to widely varying levels of compaction. At 15%AV, a PFC mixture has reached terminal density, but a dense graded mixture has a significant amount of compaction remaining. To resolve this difficulty in comparing the different mixtures, the %AV data for each sample was normalized to remove the effect of sample %AV differences.

To normalize the compaction curve data, the %AV at each gyration in a compaction was divided by the %AV after the first gyration. This way, every curve begins at the same value of 1. Logarithmic trendlines were again fit to the data to arrive at a slope and intercept that describe the curve. Figure 23 shows the equation and $R^2$ for both curves. Again, the $R^2$ values are very high.

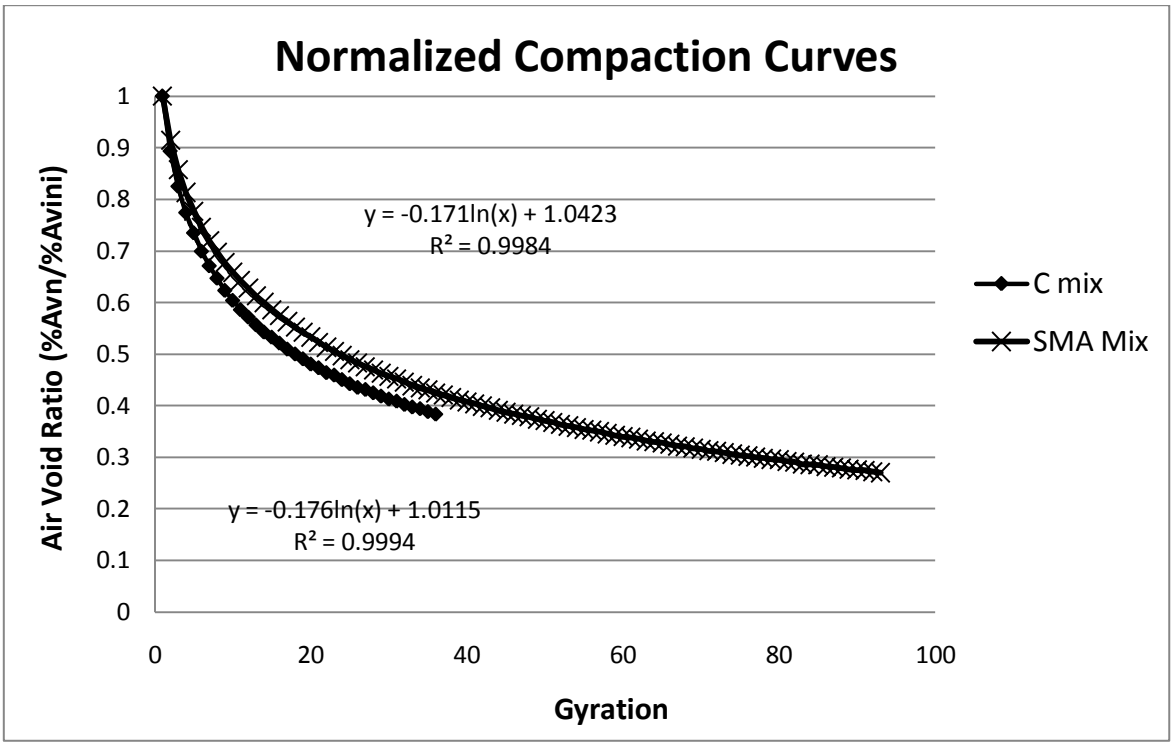


**Figure 23. Normalized Compaction Curves**

Figure 24 shows the same data but with the x-axis in logarithmic scale. The logarithmic equation was found to fit all the compaction curves very well with $R^2$ values normally above 0.99.

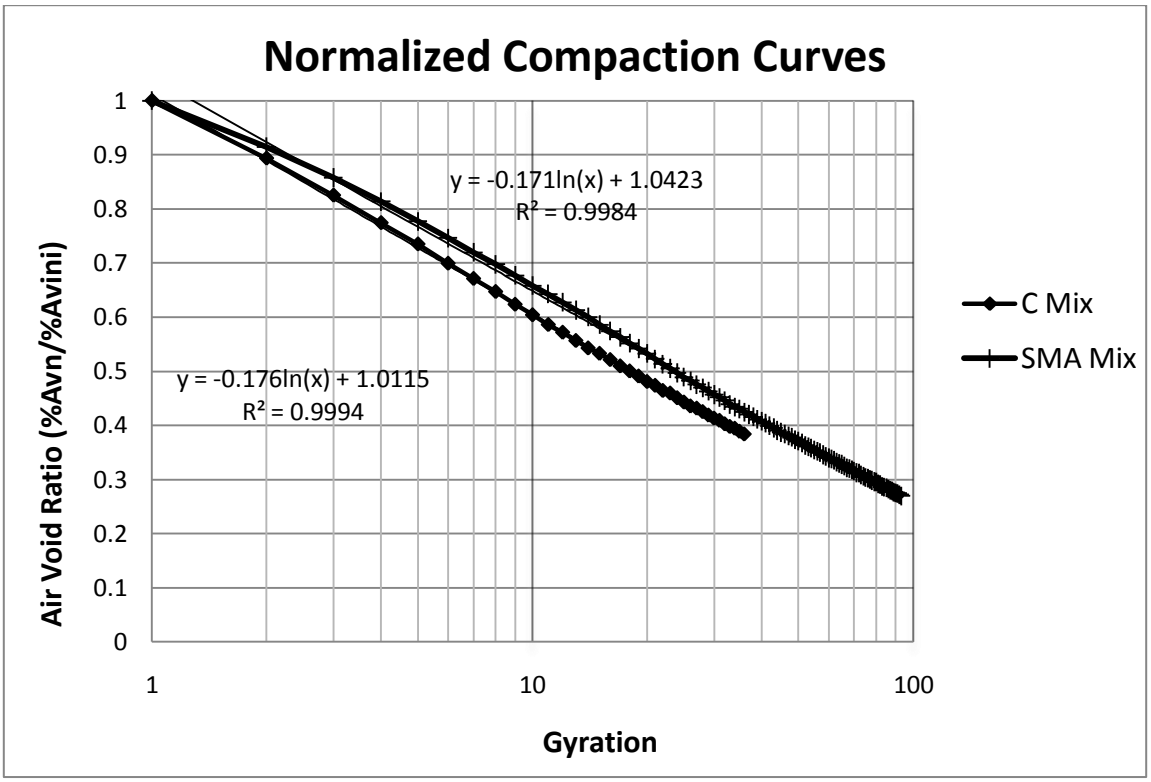


**Figure 24. Normalized Compaction Curves, Log Axis**

The slope of these logarithmic curves was chosen to be the compaction parameter *a*. The parameter *a* provides an accurate quantitative description of the overall shape of the curve and ranges from -0.11 to -0.24. The y-axis intercept is identified as parameter *c* and ranges from 1.053 to 0.987. Because the curves were normalized by their initial %AV, the *c* parameter (y-axis intercept) was almost one for every curve.

The %AV content after the first gyration was chosen as a third compaction parameter (AV $N_{ini}$). This parameter might be influenced by the aggregate gradation and binder content. In the mixtures evaluated in the study, AV $N_{ini}$ ranged from 0.16 to 0.31.

Table 6 contains compaction parameters *a*, *c*, and *AV* $N_{ini}$ for one of the four replicate samples of ever mixture design used in the study.

**Table 6 Compaction Parameters a, c, and AV $N_{ini}$**

| Mixture Name, Type | *a* | c | AV $N_{ini}$ |
|---|---|---|---|
| US 87 C | -0.176 | 1.011 | 0.183 |
| HW 6 SMA_D | -0.171 | 1.042 | 0.267 |
| SH 44 B | -0.175 | 1.010 | 0.182 |
| SH 21 C | -0.166 | 1.013 | 0.205 |
| Lufkin CAM 7.0% 70-22 | -0.176 | 1.015 | 0.208 |
| Lufkin CAM 7.5% 70-22 | -0.207 | 1.014 | 0.188 |
| Lufkin CAM 8.0% 70-22 | -0.227 | 1.013 | 0.165 |
| Lufkin CAM 7.5% 76-22 | -0.196 | 1.015 | 0.191 |
| Lufkin CAM 8.0% 76-22 | -0.223 | 1.014 | 0.179 |
| Lufkin CAM 8.5% 76-22 | -0.240 | 1.010 | 0.161 |
| Mopac SMA_C | -0.225 | 1.028 | 0.205 |
| Bryan C | -0.169 | 1.013 | 0.209 |
| SS3111_CAM | -0.208 | 1.018 | 0.193 |
| I-35 Waco SMA_D | -0.203 | 1.053 | 0.237 |
| SH 36 D | -0.153 | 0.994 | 0.238 |
| US 259 C | -0.197 | 1.015 | 0.174 |
| 341 C | -0.185 | 1.021 | 0.209 |
| 346 SMA | -0.204 | 1.052 | 0.222 |
| 342 PFC | -0.112 | 1.008 | 0.315 |
| 340 B | -0.167 | 1.015 | 0.196 |
| Arash4 C | -0.159 | 0.987 | 0.193 |
| Arash9 D | -0.159 | 0.997 | 0.223 |

While a logarithmic equation fits the compaction curves very well, the fit was not perfect. Often the most noticeable error occurred near the beginning of compaction in the first few gyrations. There was a possibility that this deviation from the logarithmic

equation could be related to a mixture property that has influence primarily early in the compaction process. In an attempt to characterize this early compaction, a linear trendline was fit through only the first five gyrations. The slope of this linear trendline was designated as *m1*. Figure 25 shows a sample compaction curve and parameter *m1*.

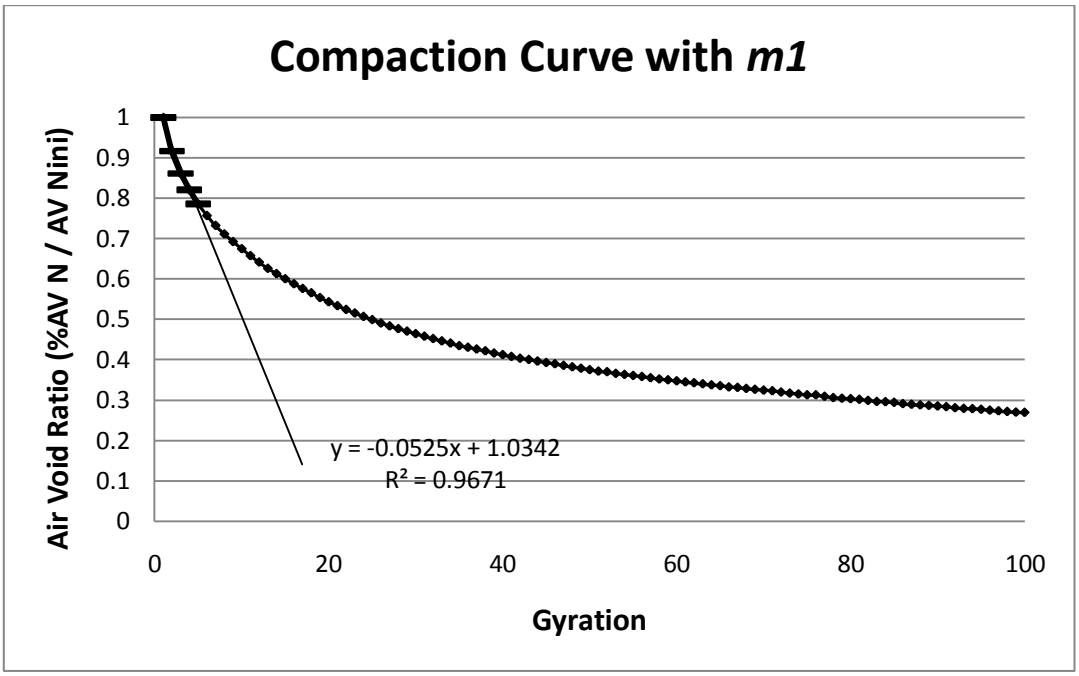


**Figure 25. Compaction Curve Showing m1**

Parameter *m1* is meant to characterize the early part of sample compaction. To characterize the later part of compaction, another linear trendline was fit through gyration numbers 96 through 100. While compacting samples, some mixtures required fewer than 100 gyrations; in these cases, the logarithmic equation was used to predict %AV at gyrations 96 through 100. A linear trendline was then fit through these

predicted gyration points. The slope of this trendline is designated as parameter *m2*. Figure 26 shows *m2* and a compaction curve.

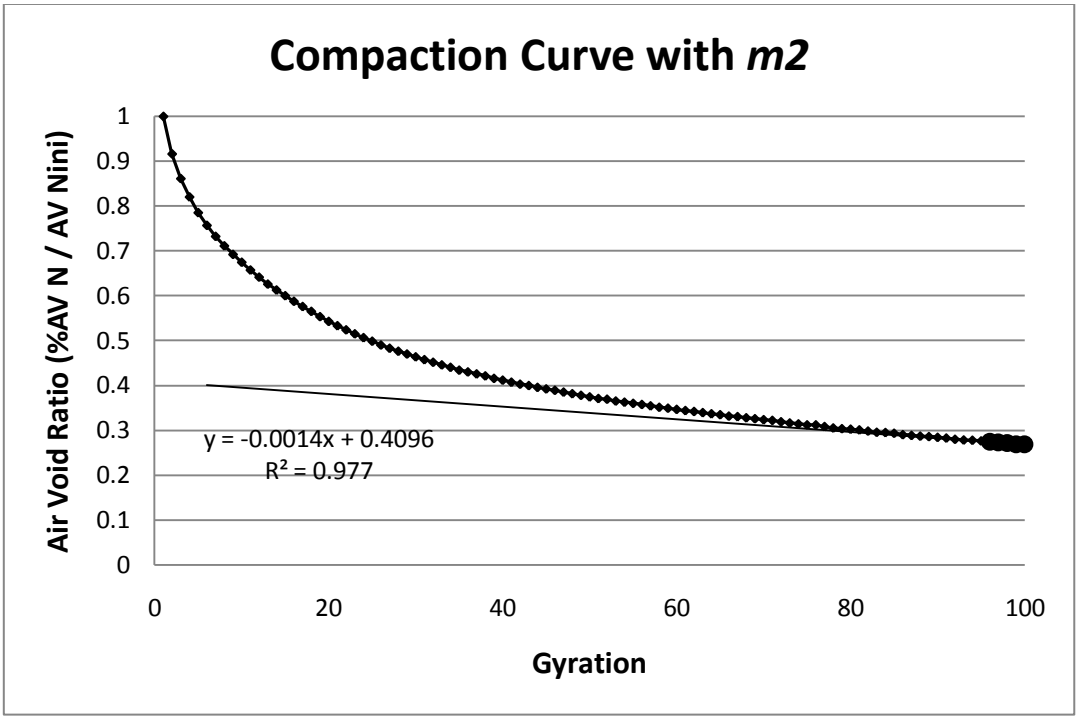


**Figure 26. Compaction Curve Showing m2**

Another compaction parameter was *Δ Slope*. It is the absolute value of the difference between *m1* and *m2*. The last parameter α was chosen to be the gyration number where the trendlines created for *m1* and *m2* intersect. Figure 27 shows the trendlines used to find *m1* and *m2*; the point where these two lines intersect is parameter α.

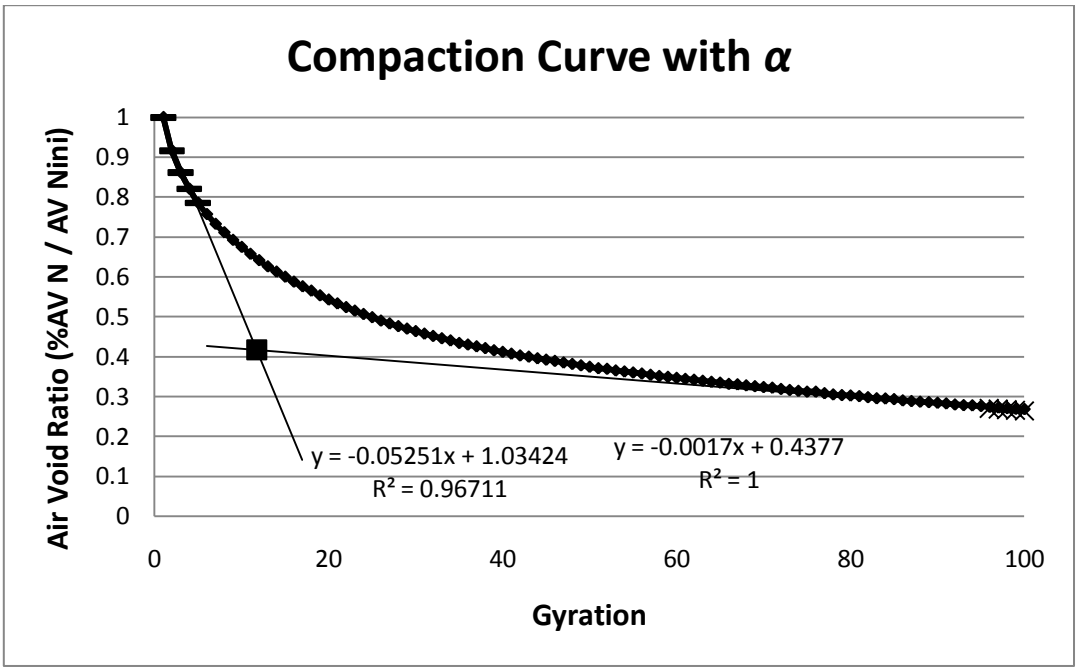


**Figure 27. Compaction Curve Showing Parameter α**

It was hoped that these seven compaction parameters could not only characterize the broad shape of the compaction curves but also isolate some of the subtle differences in compaction performance. Table 7 contains parameters *m1, m2, α,* and *Δ Slope* for one replicate sample of every mixture design used in the study.

**Table 7 Compaction Parameters m1, m2 α, and Δ Slope**

| Mixture Name, Type | *m1* | *m2* | *α* | *Δ Slope* |
|---|---|---|---|---|
| US 87 C | -0.065 | -0.0018 | 10.455 | 0.063 |
| HW 6 SMA_D | -0.055 | -0.0017 | 11.475 | 0.053 |
| SH 44 B | -0.065 | -0.0018 | 10.351 | 0.064 |
| SH 21 C | -0.061 | -0.0017 | 10.524 | 0.059 |
| Lufkin CAM 7.0% 70-22 | -0.064 | -0.0018 | 10.522 | 0.062 |
| Lufkin CAM 7.5% 70-22 | -0.076 | -0.0021 | 10.453 | 0.074 |
| Lufkin CAM 8.0% 70-22 | -0.085 | -0.0023 | 10.337 | 0.082 |
| Lufkin CAM 7.5% 76-22 | -0.072 | -0.0020 | 10.481 | 0.070 |
| Lufkin CAM 8.0% 76-22 | -0.083 | -0.0023 | 10.388 | 0.080 |
| Lufkin CAM 8.5% 76-22 | -0.091 | -0.0025 | 10.194 | 0.089 |
| Mopac SMA_C | -0.078 | -0.0023 | 10.960 | 0.075 |
| Bryan C | -0.061 | -0.0017 | 10.538 | 0.060 |
| SS3111_CAM | -0.075 | -0.0021 | 10.586 | 0.073 |
| I-35 Waco SMA_D | -0.064 | -0.0021 | 11.610 | 0.062 |
| SH 36 D | -0.058 | -0.0016 | 10.429 | 0.057 |
| US 259 C | -0.072 | -0.0020 | 10.493 | 0.070 |
| 341 C | -0.065 | -0.0019 | 10.709 | 0.064 |
| 346 SMA | -0.063 | -0.0021 | 11.738 | 0.061 |
| 342 PFC | -0.038 | -0.0011 | 11.253 | 0.037 |
| 340 B | -0.060 | -0.0017 | 10.616 | 0.059 |
| Arash4 C | -0.064 | -0.0016 | 9.900 | 0.063 |
| Arash9 D | -0.061 | -0.0016 | 10.366 | 0.059 |

# CHAPTER III

# STATISTICAL ANALYSIS OF THE RELATIONSHIP BETWEEN MIXTURE CHARACTERISTICS AND COMPACTION PARAMETERS

Following the mixture and compaction data collection phase of the project, statistical analyses were completed on the compiled data. The analysis has three main parts. The goal of the first part was to use a number of factors analysis to determine how many of the seven mixture properties and seven compaction parameters are required to reproduce the correlation matrix of the measurements to a reasonable and repeatable approximation. In the second part of the analysis, a Neural Net was used as a first step in determining an upper bound on the correlation between the mixture and compaction data. The third part employed a stepwise regression analysis to determine which of the mixture properties are needed to efficiently predict the compaction parameters.

## FACTOR ANALYSIS

There were seven compaction parameters and seven mixture properties considered in the study, but there is no guarantee that each one is necessary or useful. It is possible that some of the mixture parameters chosen have no correlation with compaction. These are parameters that will not contribute to the model and should be excluded. It is also possible for two parameters to closely correlate with each other. In

that case, only one of them can be used as a surrogate for both because the other does not provide any unique or additional information to improve the model.

For this study the Number of Factors command in the PLS toolbox in Matlab was utilized (Matlab 7.4 2007). The algorithm used in the program has been tested using data from a variety of fields and is a trusted tool for estimating the number of factors in a problem (Henry 1999). The Number of Factors analysis indicated that of the seven mixture parameters, only four were important, and of the seven compaction parameters, only two were important.

While the Number of Factors tool does a good job of estimating how many important variables there are by finding which factors have the most variability, it does not provide information about what variables are important for prediction. Because the compaction curves were fit so well by a logarithmic equation, it was decided that the parameters $a$ and $AV\,N_{ini}$ used to produce that normalized curve were likely the most important. The y-axis intercept of the equation, $c$ diminished in importance because normalizing the data forced $c$ to equal very near 1. The other parameters were basically derived from the curve and were meant to characterize differences between the actual data curve and the trendline. Since the data were fit so well by the trendline, the other parameters carried little weight. This conclusion was later backed up by regression analysis.

The Number of Factors algorithm found that there were four important mixture properties. As in the case of the compaction parameters, this only means that most of the variability was found in four factors, not that there are four variables needed to

predict compaction. It was much harder to intuitively tell which mixture properties were important. It was also possible that four properties important in predicting *a* might be different than the four needed for $AV\,N_{ini}$. For these reasons it was decided to include all original mixture properties in further analyses.

One other tool was used to determine the number of important factors: the Principal Components analysis in the statistics program JMP. Given a set of original variables, a number of principal components are formed. The first principal component is the linear combination of the standardized original variables that has the greatest variance. Each subsequent component is the linear combination of the standardized original variables that has the greatest possible variance and is uncorrelated with all previously defined components (SAS, 2008). The two ways to use these to estimate the number of principal components are: (1) determine how many components are needed to capture most of the variability in the data set and (2) find the component number where there is a bend in the scree plot.

The Principal Component analysis was first performed on the compaction parameter data. Table 8 shows the seven components sorted by their importance. The eigenvalue for each component is displayed in the second column, and the third shows the percent of variation in the data that is contained in each component. A great deal of the variability (97%) is captured by just two principal components. Figure 28 shows a scree plot of this data. A scree plot graphs the number of components versus the eigenvalue for each component. Common practice is to choose the number of

components where there is a bend in the plot. This would indicate that there are three principal components.

**Table 8 Principal Component Analysis Results for Compaction Parameters**

**Principal Components: on Correlations**

| Number | Eigenvalue | Percent | Percent | Cum Percent |
|---|---|---|---|---|
| 1 | 4.6438 | 66.340 | | 66.340 |
| 2 | 2.1688 | 30.982 | | 97.322 |
| 3 | 0.1347 | 1.924 | | 99.246 |
| 4 | 0.0511 | 0.730 | | 99.976 |
| 5 | 0.0017 | 0.024 | | 100.000 |
| 6 | 0.0000 | 0.000 | | 100.000 |
| 7 | -0.0000 | -0.000 | | 100.000 |

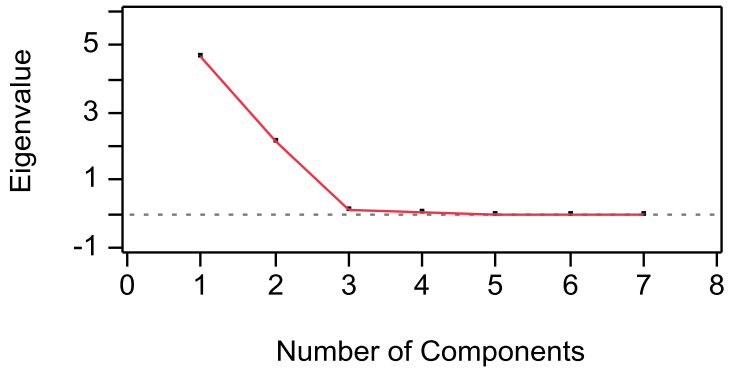


**Figure 28. Scree Plot for Compaction Parameters**

When this analysis is applied to the mixture property data the results are a little less clear. There is no definite bend in the scree plot and when examining the eigenvalues and their percentages, it is up to the user's interpretation to decide how many are important. Four components would capture 93% of the variability while five would capture 97%. Table 9 shows the variability captured for each number of variables and Figures 29 shows a scree plot of this data.

**Table 9 Principal Component Analysis Results for Mixture Properties**

| Principal Components: on Correlations | | | | |
|---|---|---|---|---|
| **Number** | **Eigenvalue** | **Percent** | **Percent** | **Cum Percent** |
| 1 | 2.9239 | 41.770 | | 41.770 |
| 2 | 1.9042 | 27.203 | | 68.972 |
| 3 | 1.0563 | 15.090 | | 84.063 |
| 4 | 0.6419 | 9.170 | | 93.232 |
| 5 | 0.2883 | 4.119 | | 97.351 |
| 6 | 0.1314 | 1.877 | | 99.228 |
| 7 | 0.0540 | 0.772 | | 100.000 |

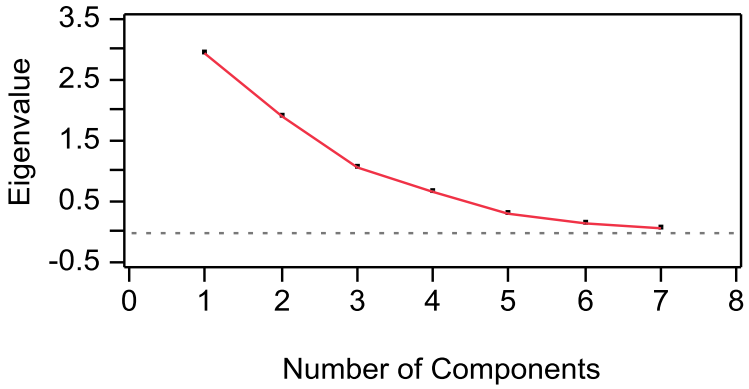


**Figure 29. Scree Plot for Mixture Properties**

The results of these two analyses were slightly different, but can be interpreted to arrive at the same conclusion. For further analyses, four or five mixture properties and two compaction parameters will be considered.

## NEURAL NET ANALYSIS

The second part of the analysis used a Neural Net as a first step to determine if there is a correlation between the data. The important parameters found in the previous

step can be identified with this type of analysis. A neural net is a valuable tool modeled `after nerve cells in the brain that can efficiently model different response surfaces. It uses a flexible network of functions of input variables to predict responses. Figure 30 shows an illustration of the intermediate variables used in a neural net analysis. Its strength is that it can approximate any surface to any accuracy given enough hidden nodes. Its drawbacks are that it tends to over-fit data and its results are hard to interpret. The program may find a correlation between two data sets, but it could be difficult to determine what the correlation is.

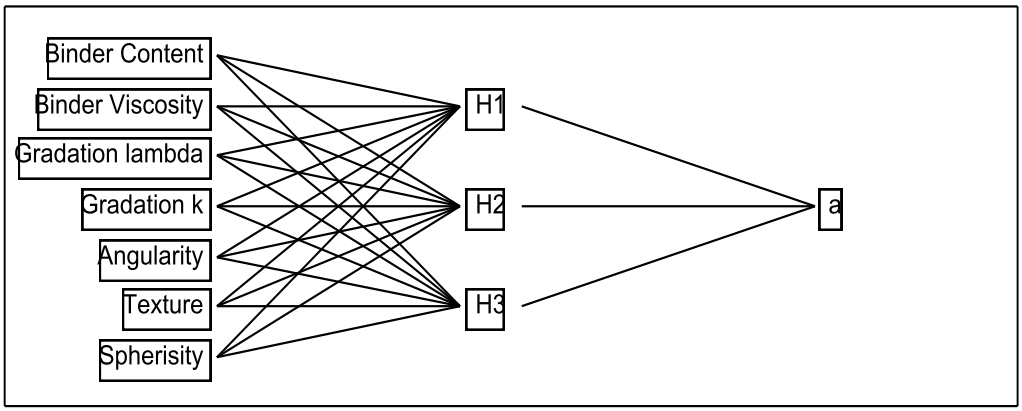


**Figure 30. Neural Net Illustration for *a***

The statistics program JMP was used for the neural net analysis. Neural nets have a tendency to over-fit the data used to create a model (training data). For this reason it is necessary to include cross-validation in the neural net analysis. K-fold cross-validation was used. This means that the data were first fit using every data point. Then

a portion of the training set was excluded and the model was run again. The solution from this second run was applied to the withheld data and the $R^2$ of that fit recorded. This process will be repeated K times with different excluded data sets and the $R^2$ from all K times were averaged. The user defines K, the number of runs included in the analysis. This tool helps determine if the model does a good job of fitting the data and at predicting new data, or if it only fits the training data well but does a poor job predicting.

In the first attempts at this analysis, a Gauss Newton method was used with three hidden nodes and 5-fold cross-validation and the entire data set was used, replicate samples included. This produced excellent results for both compaction parameters. Table 10 shows the $R^2$ results for the analysis using all data and the cross-validated (CV) analysis. In both cases the initial $R^2$ is above 0.98 and the CV $R^2$ is also high. Figures 31 and 32 show the predicted plot for both parameters. These results show evidence that the model does a very good job at both fitting a training set of data and predicting new data.

**Table 10 Fit History for Neural Net Analyses**

| **Fit History** | | |
|---|---|---|
| | **RSquare** | **CV RSquare** |
| Entire Data Set Analysis for *a* | 0.98764 | 0.97725 |
| Entire Data Set Analysis for $AV\,N_{ini}$ | 0.98564 | 0.95136 |
| Partial Data Set Analysis for *a* | 0.99288 | 0.02280 |
| Partial Data Set Analysis for $AV\,N_{ini}$ | 0.99532 | 0.48788 |

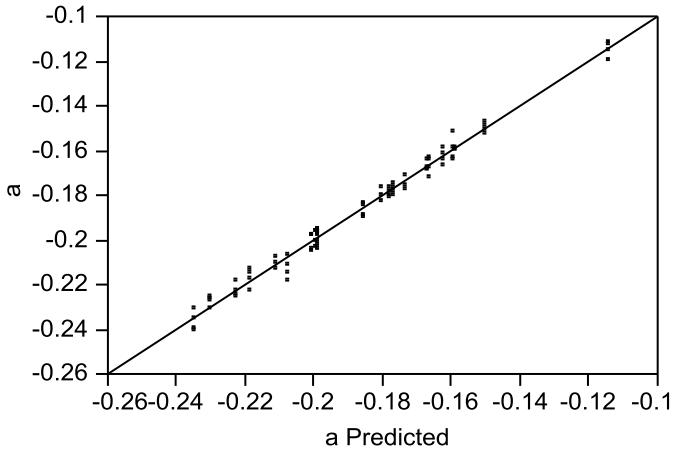


**Figure 31. Predicted Plot of CV Neural Net of Entire Data Set for *a***

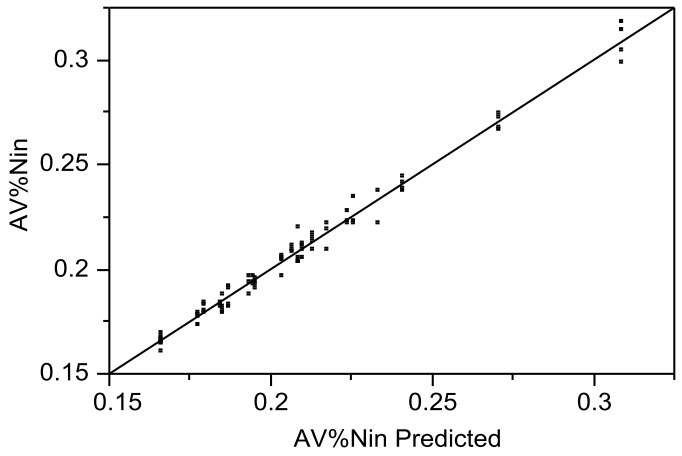


**Figure 32. Predicted Plot of CV Neural Net of Entire Data Set for $AV\,N_{ini}$**

When running the cross-validation, parts of the training set were excluded from the analysis and then predicted using the model. The results show that the model is successful at predicting these excluded points, but because there were four replicate samples for every mixture, when some points were taken out, replicate samples of the excluded points still remained in the training set. In every case, the compaction parameters for all four replicate samples very closely matched each other. This means that when one point was removed from the training set, a near copy of it remained and was used for the model. That is why the analysis resulted in such high CV $R^2$ values.

To resolve this issue, the analysis was rerun with all replicate samples taken out. Table 10 also contains the analysis results from the partial data sets. As in the previous analyses, the $R^2$ for the entire data set is very high, but excluding the replicate samples had a profound effect on the CV $R^2$. In the case of parameter *a*, the CV $R^2$ dropped to nearly zero. For $AV\,N_{ini}$, it dropped below 0.5. When doing cross-validation, the

program randomly excludes parts of the data but not the same parts every time the model is run. Because of this, the model can produce different CV $R^2$ values each time the model is run. After running the model several times, CV $R^2$ for *a* stayed very near zero, but for $AV\ N_{ini}$ it ranged from about 0.1 to 0.6. These results mean that fitting the model to certain types of mixtures and using the model to predict another type that is not within the mixture used in the fitting is not a good use of the model. The model can be used to describe the compaction parameters of mixture types that are included in the fitting or analysis.

## REGRESSION ANALYSIS

The neural net analysis showed us that the mixture property data can be fit to the compaction parameters. It also showed that there could be a problem in using the data to predict new data. The next step is to analyze the data with a different type of model whose output is easier to interpret.

The third part of the statistical analysis included a stepwise regression analysis to determine which variables best predict the compaction parameters. This analysis can be used first to find which variables are unique and which are simply related to another variable.

A stepwise analysis operates in one of two ways, forward or backward. In the first step of a forward analysis, the most significant term is entered into the model and an $R^2$ value of the fit is calculated. In the second step, the next most significant term that

improves the fit is added to the model. Each additional term must be significant at a user defined level (probability to enter). This continues until all available terms have been added or additional terms fail to exceed the entry criteria. In a backward analysis, all terms are included in the model from the beginning. In the first step, the regressor that affects the fit the least is removed provided the term is not significant at the user defined level (probability to leave). The two defined significance levels can be manipulated so that the analysis utilizes the same number of terms for forward and backward analyses.

The forward stepwise analysis was first applied to the compaction parameter *a*. Tables 11 and 12 show the step history and current estimate of the forward analysis. The step history (Table 11) outlines the order in which each parameter was added or removed from the model, and the current estimate (Table 12) provides information about the model at the last step. The four properties that the forward analysis chose were angularity, texture, sphericity, and binder viscosity. These produced a fit with an $R^2$ of 0.61. Tables 13 and 14 show the step history and current estimate for the backward analysis. This time the properties chosen were binder content, $\lambda$, *k*, and angularity. These properties produced a model with a much better $R^2$ of 0.78. It is important to note how much the accuracy of the models change as terms are removed in Table 13.

**Table 11. Forward Step History for *a***

| **Step History** | | | | | | | |
|---|---|---|---|---|---|---|---|
| **Step** | **Parameter** | **Action** | **"Sig Prob"** | **Seq SS** | **RSquare** | **Cp** | **p** |
| 1 | Angularity | Entered | 0.0000 | 0.031644 | 0.4312 | 151.19 | 2 |
| 2 | Texture | Entered | 0.0000 | 0.007502 | 0.5335 | 110.91 | 3 |
| 3 | Sphericity | Entered | 0.0035 | 0.003332 | 0.5789 | 94.134 | 4 |
| 4 | Binder Viscosity | Entered | 0.0119 | 0.00228 | 0.6100 | 83.284 | 5 |

**Table 12. Forward Stepwise Current Estimate for *a***

| Current Estimates | | | | | | | |
|---|---|---|---|---|---|---|---|
| **SSE** | **DFE** | **MSE** | **RSquare** | **RSquare Adj** | **Cp** | **AICc** | |
| 0.0286203 | 83 | 0.0003448 | 0.6100 | 0.5912 | 83.284308 | -443.956 | |
| **Lock** | **Entered** | **Parameter** | **Estimate** | **nDF** | **SS** | **"F Ratio"** | **"Prob>F"** |
| X | X | Intercept | 0.05923656 | 1 | 0 | 0.000 | 1 |
| | | Binder Content | 0 | 1 | 0.000401 | 1.166 | 0.28349 |
| | X | Binder Viscosity | 3.45322e-5 | 1 | 0.00228 | 6.613 | 0.01191 |
| | | Gradation lambda | 0 | 1 | 0.000371 | 1.076 | 0.30271 |
| | | Gradation k | 0 | 1 | 0.000838 | 2.473 | 0.1197 |
| | X | Angularity | -3.3438e-5 | 1 | 0.016441 | 47.679 | 9.3e-10 |
| | X | Texture | -0.000062 | 1 | 0.00262 | 7.599 | 0.00718 |
| | X | Sphericity | -0.2202642 | 1 | 0.004013 | 11.637 | 0.001 |

**Table 13. Backward Stepwise History for *a***

| Step History | | | | | | | |
|---|---|---|---|---|---|---|---|
| **Step** | **Parameter** | **Action** | **"Sig Prob"** | **Seq SS** | **RSquare** | **Cp** | **p** |
| 1 | Sphericity | Removed | 0.1676 | 0.000344 | 0.8018 | 7.9393 | 7 |
| 2 | Binder Viscosity | Removed | 0.0682 | 0.000613 | 0.7935 | 9.3947 | 6 |
| 3 | Texture | Removed | 0.1467 | 0.000397 | 0.7881 | 9.6304 | 5 |

**Table 14. Wackward Stepwise Current Estimate for *a***

| Current Estimates | | | | | | | |
|---|---|---|---|---|---|---|---|
| **SSE** | **DFE** | **MSE** | **RSquare** | **RSquare Adj** | **Cp** | **AICc** | |
| 0.0155502 | 83 | 0.0001874 | 0.7881 | 0.7779 | 9.6304155 | -497.639 | |
| **Lock** | **Entered** | **Parameter** | **Estimate** | **nDF** | **SS** | **"F Ratio"** | **"Prob>F"** |
| X | X | Intercept | -0.0406065 | 1 | 0 | 0.000 | 1 |
| | X | Binder Content | -0.019771 | 1 | 0.015063 | 80.397 | 7.6e-14 |
| | | Binder Viscosity | 0 | 1 | 0.000158 | 0.839 | 0.36224 |
| | X | Gradation lambda | -0.0119215 | 1 | 0.016959 | 90.520 | 6.1e-15 |
| | X | Gradation k | 0.09735515 | 1 | 0.025651 | 136.911 | 3e-19 |
| | X | Angularity | -1.9922e-5 | 1 | 0.00236 | 12.597 | 0.00064 |
| | | Texture | 0 | 1 | 0.000397 | 2.147 | 0.14669 |
| | | Sphericity | 0 | 1 | 0.000471 | 2.563 | 0.11321 |

Stepwise regression does not always produce the same result forwards and backwards, so this difference is no surprise. The backward analysis result is chosen as the better one because of its higher $R^2$ value.

The same two types of stepwise regression were performed for the compaction parameter $\%AVN_{ini}$. This time the forward and backward analyses arrived at the same four properties for the model. Table 15 shows the step history of both analyses. Steps one through four are from the forward analysis; steps five through seven are from the backward analysis. Table 16 shows the current estimate of the analysis. Binder content, *k*, sphericity, and texture were the important properties for $\%AVN_{ini}$. This model has an $R^2$ value of 0.80.

**Table 15. Stepwise History for $\%AVN_{ini}$**

**Step History**

| Step | Parameter | Action | "Sig Prob" | Seq SS | RSquare | Cp | p |
|---|---|---|---|---|---|---|---|
| 1 | Gradation k | Entered | 0.0000 | 0.053354 | 0.5454 | 108.8 | 2 |
| 2 | Binder Content | Entered | 0.0000 | 0.01599 | 0.7089 | 41.47 | 3 |
| 3 | Sphericity | Entered | 0.0000 | 0.008431 | 0.7951 | 6.9139 | 4 |
| **4** | Texture | Entered | 0.0150 | 0.001386 | **0.8093** | 2.9029 | 5 |
| 5 | Binder Viscosity | Removed | 0.7528 | 0.000023 | 0.8112 | 6.0999 | 7 |
| 6 | Gradation lambda | Removed | 0.5547 | 8.025e-5 | 0.8103 | 4.4479 | 6 |
| **7** | Angularity | Removed | 0.4978 | 0.000105 | **0.8093** | 2.9029 | 5 |

**Table 16. Stepwise Current Estimate for $\%AVN_{ini}$**

| Current Estimates | | | | | | | | |
|---|---|---|---|---|---|---|---|---|
| | | SSE | DFE | MSE | RSquare | RSquare Adj | Cp | AICc |
| | | 0.018658 | 83 | 0.0002248 | 0.8093 | 0.8001 | 2.9028977 | -481.606 |
| **Lock** | **Entered** | **Parameter** | | **Estimate** | **nDF** | **SS** | **"F Ratio"** | **"Prob>F"** |
| X | X | Intercept | | 0.48625387 | 1 | 0 | 0.000 | 1 |
| | X | Binder Content | | -0.0111538 | 1 | 0.009379 | 41.724 | 6.75e-9 |
| | | Binder Viscosity | | 0 | 1 | 4.127e-7 | 0.002 | 0.96613 |
| | | Gradation lambda | | 0 | 1 | 0.000061 | 0.269 | 0.60569 |
| | X | Gradation k | | 0.06574747 | 1 | 0.030723 | 136.671 | 3.2e-19 |
| | | Angularity | | 0 | 1 | 0.000105 | 0.464 | 0.49778 |
| | X | Texture | | -4.5366e-5 | 1 | 0.001386 | 6.167 | 0.01503 |
| | X | Sphericity | | -0.3873268 | 1 | 0.008991 | 39.995 | 1.22e-8 |

Reviewing these results, it is clear that using four of the seven mixture properties produces an efficient model of the compaction parameters. Modeling *a* requires the mixture properties binder content, $\lambda$, *k*, and angularity. The form of the model equation is shown in Equation 4.

$$a = -4.06 \times 10^{-2} + (-1.98 \times 10^{-2} \times Binder\ Content) + (-1.19 \times 10^{-2} \times \lambda) + (9.74 \times 10^{-2} \times k) + (-1.99 \times 10^{-5} \times Angularity) \quad (4)$$

Modeling $\%AV\,N_{ini}$ requires the mixture properties binder content, *k*, spherisity, and texture. The form of this model is shown in Equation 5.

$$\%AV\ Nini = 4.86 \times 10^{-1} + (-1.12 \times 10^{-2} \times Binder\ Content) + (6.57 \times 10^{-2} \times k + -4.54 \times 10 - 5 \times Texture + -3.87 \times 10 - 1 \times Sphericity \quad (5)$$

It is important to test the prediction capabilities of the regression model for new data. To do this, a portion (20%) of the training data set was removed, and the model

was rerun with the limited data set. Then, the new model was used to predict the compaction parameters of the mixtures that were excluded. This gave an indication of how well the model performs with new data.

Figures 33 and 34 show the results of this analysis. A model was created with an abridged data set and then used to predict the excluded data points. The reintroduced points are denoted by red circles. The results of this analysis change depending on which portion of the data set is withheld. In the case of Figure 33, a model to predict *a* was created using four mixture parameters (binder content, λ, *k*, angularity) and produced an $R^2$ of 0.81. When the excluded points were reintroduced, the $R^2$ dropped to 0,65. In Figure 33, the red circles are noticeably astray as compared to the trendline. In the case of Figure 34 and $AV\%N_{ini}$, the $R^2$ fell from 0.83 to 0.78.

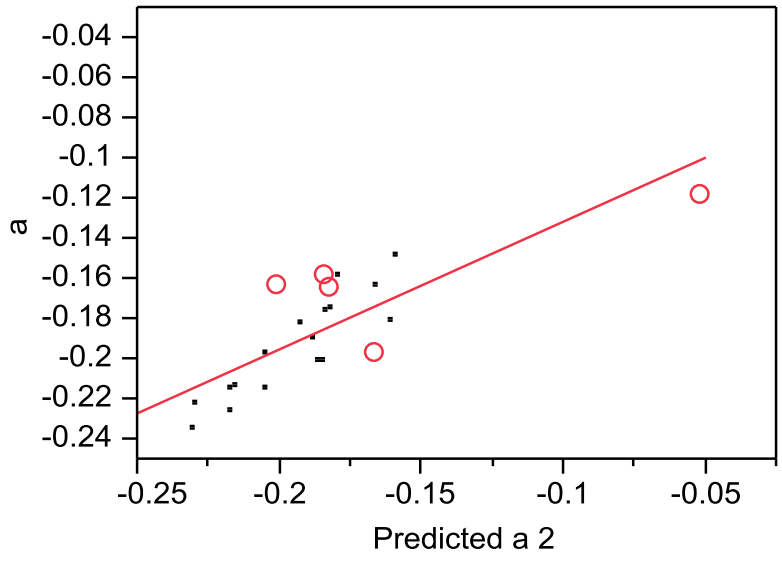


**Figure 33 *a* versus Predicted *a***

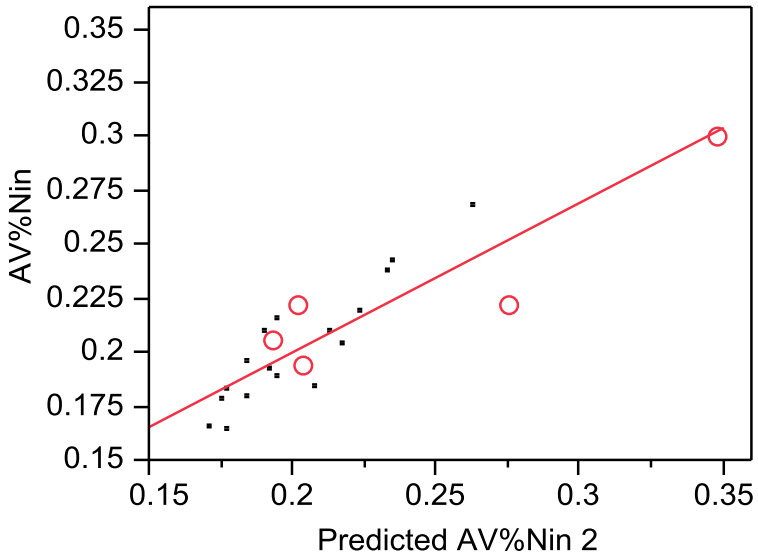


**Figure 34 *%AVN$_{ini}$* versus Predicted *%AVNin***

This analysis was repeated several times used different sets of excluded data each time. The prediction performance of the model tended to depend on what data were excluded. If one mixture from each of the major mixture types was excluded, the model performed well because the training set still included mixtures similar to the ones taken out. When all mixtures of a specific mixture type were excluded, the model performed worse because there were no mixtures similar to the ones excluded left in the training set. These results affirm that the model is successful at predicting compaction parameters for new mixtures that are similar to ones included in the initial data set. For mixtures that are much different than the mixtures included in the model, the performance is diminished.

## SUMMARY AND VALIDATION

The factor analysis showed that of the 14 possible parameters included in the study, four mixture properties were important, and two compaction parameters were important. It indicated how many variables were important but it did not identify these important variables.

The neural net analysis showed that it was possible to fit the compaction parameters using the mixture properties to a high degree of accuracy.

The stepwise regression analysis confirmed that four properties prodiced a good fit, and it identified which four were the important terms. These results from the neural net and the regression analysis showed that fitting the model to certain types of mixtures and using the model to predict anather types that is not within the mixtures used in the fitting is not a good use of the model. The model can be used to describe the compaction parameters of mixture types that are included in the fitting or analysis

# CHAPTER IV

# CONCLUSIONS AND FUTURE WORK

The statistical analysis of the seven mixture properties and seven compaction parameters resulted in two, four-term regression equations (Equations 4 and 5) that can be used to predict the compaction parameters of HMA mixtures (*a* and $\%AVN_{ini}$). The analysis showed that these equations accurately fit the data in the training set. They can also successfully predict compaction parameters for new mixtures provided they are similar to mixtures included in the model. Parameters for mixtures unlike those included in the model were not predicted well. It is possible that by enlarging the models data set, parameters for most types of mixtures could be predicted.

In addition to the prediction capabilities of the equations, there are other notable results from the study. By examining the form of the equations and the terms used, some qualitative conclusions can be drawn from the results. Out of the seven original material properties included in the study, both equations require only four properties, but all four were not the same for both equations. The important properties for predicting *a* are aggregate gradation parameters *k* and λ, binder content, and aggregate angularity. The properties for predicting $\%AVN_{ini}$ are *k*, binder content, and aggregate sphericity and texture.

Compaction parameter *a* is the slope of a logarithmic trendline fit to the normalized compaction curve. Typical values range from around -0.1 to -0.25. A more negative slope corresponds with greater compactability; the sample compacts at a higher

rate. The equation reveals the attributes that contribute to a more negative compaction slope. A low *k*, high λ, high binder content, and high angularity are shown to aid compaction. Gradations with lower *k* values have a lower slope and indicate a dense gradation; gradations with higher *k* values have higher slopes and are said to be more open or gap graded. Gradations with higher λ values have coarser aggregate gradation; lower values indicate finer gradations. The binder in an HMA mixture acts as a lubricant between aggregate particles during compaction, and the aggregate angularity affects how aggregates shift around each other during compaction. HMA mixtures with dense gradations, larger coarse aggregate, and high binder contents should be easily compacted. It is possible that the increase in angularity improves the locking between the particles and reduces slipping; hence and increase in angularity improves the transfer of stresses and compactability of the mixture.

The second compaction parameter $\%AVN_{ini}$ is an estimation of the %AV of the sample during compaction, after the first gyration. HMA mixtures with lower %AV at the start of compaction will require fewer gyrations to reach the target %AV. Typical values range from 0.16 to 0.3. Equation 5 shows that the properties that contribute to low $\%AVN_{ini}$ are low gradation *k*, high binder content, high sphericity, and high texture. Sphericity is a measure of how round an aggregate is. Very round aggregates (nearly a sphere) have higher sphericity values than more oblong aggregates. Aggregates with rough surfaces will have higher texture values than smooth aggregates. Again, most of these property relationships agree with expectations, but the effect of high aggregate texture enhancing compactability is not completely understood.

In the future, other studies on the topic of compactability could benefit from the following changes in experimental design.

- Several additional mixtures included to the data set and a wider variety of mixtures could improve the model. Some of the inconsistencies in the statistical model could be addressed by the addition of more mixtures, and it is possible that the prediction performance could be improved as well. This study included 22 mixtures, two or three times that number would probably significantly improve the results.

- The gyratory compaction curves used in this study were fit very well by a logarithmic trendline. This trendline utilizes two parameters to describe the curve (slope and intercept). Almost any other compaction parameter used in this study or the other studies discussed in the literature review can be back-calculated to a high accuracy using those two trendline parameters. Future studies should focus on the slope and height of the compaction curve and less on other parameters that do not describe this curve.

- As a way to increase the diversity of the data set, individual properties of HMA mixtures included in a study could be changed to create a new mixture with slightly different properties. For instance, the angular and rough aggregate used

in one mixture could be replaced by a round and smooth aggregate, binders and binder contents could be changed, or aggregate gradations could be manipulated.

- It is possible that there are other mixture properties that could be good predictors of compaction that were not included in this study. Some suggestions include voids in mineral aggregate (VMA), effective binder content, and dry-rodded density of the aggregate mixture.

- By comparing the compaction parameters for each set of four replicate samples for each mixture, it was found that all replicates have nearly the same compaction parameters. This similarity of parameters between replicates adds little diversity to the model, and in some cases all replicates were left out of the analysis for simplicity. Future studies need not include replicate samples in the statistical analysis.

This study found that there are significant correlations between some mixture properties and compaction parameters. By focusing on the right mixture properties and including a large variety of HMA mixtures, a model that predicts compaction accurately should be possible.

## REFERENCES

Bennert, Thomas. (2006). *Comparing Fine Aggregate Angularity with Aggregate and Hot-Mix Asphalt Performance Tests.* Transportation Research Board of the National Academies, Washington, DC.

Delgadillo, Rodrigo. (2008). "Effects of temperature and pressure on hot mix asphalt compaction: Field and laboratory study". *Journal of Materials in Civil Engineering* © ASCE, 20(6), 440-448.

Fletcher, Thomas. (2003). "Aggregate Imaging System for Characterizing the Shape of Fine and Coarse Aggregates." *Transportation Research Record* 1832 , Transportation Research Board, Wahington, DC.

Henry, Ronald. (1999). "Comparing a new algorithm with the classic methods for estimating the number of factors." *Chemometrics and Intelligent Laboratory Systems*, 48(1), 91-97.

Huang, Baoshan. (2009). "Effects of coarse aggregate angularity and asphalt binder on laboratoryoratory-measured permanent deformation properties of HMA." *International Journal of Pavement Engineering*, 10(1), 19-28.

Khan, Z.A. (1998). "Comparative study of asphalt comcrete laboratoryoratory compaction methods to cimulate field compaction." *Construction and Building Materials* 12, 373-384.

Lee, Soon-Jae. (2008). "The effects of compaction temperature on CRM mixtures made

with the SGC and Marshall compactor." *Construction and Building Materials* 22, 1122-1128.

Leiva, Fabricio. (2008). *Analysis of Hot-Mix Asphalt Laboratory Compactability Using Laboratory Compaction Parameters and Mix Characteristics.* Trasportation Research Board of the National Academies, Washington, DC.

Mahmoud, Enad. (2010). "Comprehensive evaluation of AIMS texture, angularity, and dimension measurements." *Journal of Materials in Civil Engineering*. 22(4), 369-379

Matlab Software Version 7.4 (2007). (R2007a) *The Math Works*, Inc. Natick, MA.

SAS Institute Inc. (2008). *JMP® 8Statistics and Graphics Guide*. SAS Institute Inc. Cary, NC.

Stakston, Anthony D. (2002). "Effect of fine aggregate angularity on caompaction and shearing resistance of asphalt mixtures." *Transportation Research Record*, 1789, Transportation Research Board, Washington, DC.

TxDOT Designation: Tex-241-F, (2009) *Superpave Gyratory Compacting of Test Specimens of Bituminous Mixtures*. July Texas Department of Transprotation. Austin, TX,

TxDOT. (2008) *Pavement Design Guide.* Texas Department of Transportation, Austin, TX.

# APPENDIX A

## AIR VOID CORRECTION

$G_{mb}$ estimated (N) = $\frac{Mass}{\frac{\pi * D^2}{4} * h * \gamma_w}$

Correction Factor (N) = $\frac{G_{mb}\ CoreLok\ measured\ @\ N_{final}}{G_{mb} volumetrically\ estimated\ @\ N_{final}}$

$G_{mb}$ corrected (N) = $Correction\ factor\left(N_{final}\right) * G_{mb} estimated\ (N)$

%AV corrected (N) = $1 - \frac{G_{mb} corrected\ (N)}{G_{mm}}$

**APPENDIX B**

**AGGREGATE STOCKPILE CALCULATIONS**

*This is a proposed procedure and has not yet been approved.*

---

## Standard Practice for

# Determining Aggregate Source Shape Values from Digital Image Analysis Shape Properties

---

**AASHTO Designation: xx-xx**

## Standard Practice for

# Determining Aggregate Source Shape Values from Digital Image Analysis Shape Properties

## AASHTO Designation: xx-xx

### SCOPE

**This standard covers the determination of aggregate source and source blend shape characteristics using gradation analysis and shape properties determined by means of digital image analysis.**

**This standard may involve hazardous materials, operations, and equipment. This standard does not purport to address all of the safety problems associated with its use. It is the responsibility of the user of this standard to establish appropriate safety and health practices and determine the applicability of regulatory limitations prior to use.**

### REFERENCED DOCUMENTS

***AASHTO Standards*:**

- T 11 Amount of Material Finer Than 75µm in Aggregate
- T 27 Standard Method of Test for Sieve Analysis of Fine and Coarse Aggregates
- T 84 Standard Method of Test for Specific Gravity and Absorption of Fine Aggregate
- T 85 Standard Method of Test for Specific Gravity and Absorption of Coarse Aggregate
- TP XX Standard Method of Test for Determining Aggregate Shape Properties by Means of Digital Image Analysis

### TERMINOLOGY

**Aggregate size—material retained on a given sieve size after passing the next larger sieve.**

**Fine Aggregate—Aggregate material passing 4.75mm (#4) sieve.**

sieve sizes: 2.36mm (#8), 1.18mm (#16), 0.60mm (#30), 0.30mm (#50), 0.15mm (#100), 0.075mm (#200)

**Coarse Aggregate—Aggregate material retained on 4.75mm (#4) sieve.**

sieve sizes: 25.0mm (1”), 19.0mm (3/4”), 12.5mm (1/2”), 9.5mm (3/8”), 4.75mm (#4)

**Shape Properties for each retained sieve (x)**

**Gradient Angularity (*GA*)—Applies to both fine and coarse aggregate sizes and is related to the sharpness of the corners of 2-dimensional images of aggregate particles. The gradient angularity quantifies changes along a particle boundary with higher gradient values indicating a more angular shape. Gradient angularity has a relative range of 0 to 10000 with a perfect circle having a value of 0.**

Gradient Angularity: $$GA = \frac{1}{\frac{n}{3} - 1} \sum_{i=1}^{n-3} \left| \theta_i - \theta_{i+3} \right| \qquad (1)$$

where: θ angle of orientation of the edge points

*n* is the total number of points

subscript *i* denoting the i[th] point on the edge of the particle.

**Texture (or Micro-Texture) (*TX*)—Applies to coarse aggregate sizes only and describes the relative smoothness or roughness of surface features less than roughly 0.5 mm in size which are too small to affect the overall shape. Texture has a relative scale of 0 to 1000 with a smooth polished surface approaching a value of 0.**

$$TX = \frac{1}{3N} \sum_{i=1}^{3} \sum_{j=1}^{N} \left( D_{i,j}(x, y) \right)^2 \qquad (2)$$

where:

D = decomposition function

n = decomposition level

N = total number of coefficients in an image

i = 1, 2,or 3 for detailed images

j = wavelet index

x,y = location of the coefficients in transformed domain

**Sphericity (*SP*)—Applies to coarse aggregate sizes only and describes the overall three dimensional shape of a particle. Sphericity has a relative scale of 0 to 1. A sphericity value of one indicates a particle has equal dimensions (cubical).**

$$SP = \sqrt[3]{\frac{d_S * d_I}{d_L^2}} \qquad (3)$$

where: $d_S$ = particle shortest dimension

$d_I$ = particle intermediate dimension

$d_L$ = particle longest dimension

**Form 2D—Applies to fine aggregate sizes only and is used to quantify the relative form from 2-dimensional images of aggregate particles. Form2D has a relative scale of 0 to 20. A perfect circle has a Form 2D value of zero.**

$$Form2D = \sum_{\theta=0}^{\theta=360-\Delta\theta} \left[ \frac{R_{\theta+\Delta\theta} - R_{\theta}}{R_{\theta}} \right] \quad (4)$$

where: $R_\theta$ is the radius of the particle at an angle of θ

$\Delta\theta$ is the incremental difference in the angle

**Flat and Elongated—those particles having a ratio of longest dimension to shortest dimension greater than a specified value.**

Aggregate particle dimensions in an x, y, z coordinate system

$d_S$ = particle shortest dimension

$d_I$ = particle intermediate

$d_L$ = particle longest dimension

Flatness Ratio (*S/L*): $Flatness = \frac{d_S}{d_I}$ *(5)*

Elongation Ratio (*I/L*): $Elongation = \frac{d_I}{d_L}$ *(6)*

Flat and Elongated Value (F&E): $L/S = \frac{d_L}{d_S}$ *(7)*

**Flat or Elongated—those particles having a ratio of intermediate dimension to shortest dimension or longest dimension to intermediate dimension greater than a specified value.**

Flat or Elongated (ForE): $\frac{d_I}{d_S} or \frac{d_L}{d_I} > Ratio$ (i.e.: 1, 2, 3…) *(8)*

**$\%Pass_x$ = % passing sieve x**

**$\%R_x$ = % retained on sieve x (passing sieve x+1)**

---

## SIGNIFICANCE AND USE

**Shape, angularity, and surface texture of aggregates have been shown to directly affect the engineering properties of highway construction materials such as hot mix asphalt concrete, Portland cement concrete, and unbound aggregate layers. This standard is used to characterize the combined shape values for an aggregate source from the individual**

**particle shape properties determined by digital image analysis from AASHTO Test Method xx-xx. The aggregate shape characterization includes Gradient Angularity, Form 2D, Sphericity, Texture, and Flat and Elongated value.**

*Note 1*—The National Cooperative Highway Research Program Report 555 provides background information relevant to characterizing aggregate shape, texture and angularity.

**This practice may be used to characterize the shape characteristics of single source aggregate materials and multiple source aggregate material blends.**

---

## PROCEDURE

**Determine the aggregate sample grading according to AASHTO T27 and the amount finer than 75μm according to AASHTO T11.**

**Determine the aggregate sample specific gravities according to AASHTO T84 and T85.**

**Determine the material sample shape values for Form 2D, Gradient Angularity, Sphericity, Form Ratios (F&E, F or E), and Texture according to AASHTO TP XX.**

---

## CALCULATIONS – SINGLE SOURCE

**The material sample is typically characterized by individual evaluation of material retained on each sieve size, passing the next larger sieve. For the purpose of calculating the combined shape values, consider any sizes that contain inadequate percent retained mass to achieve minimum particle count to have the same shape value as the average of the next larger or the next smaller size, whichever is present.**

**Calculate the Percent Retained for the aggregate sample on each sieve using the AASHTO T27 results.:**

Sieve Sizes (x):

Coarse: 25.0mm(1”), 19.0mm(3/4”), 12.5mm(1/2”), 9.5mm(3/8”), 4.75mm(#4)

Fine: 2.36mm(#8), 1.18mm(#16), 0.60mm(#30), 0.30mm(#50), 0.15mm(#100), 0.075mm(#200)

Percent Passing: $\%Pass_x$ = % passing sieve x

Percent Retained: $\%R_x$ = % retained on sieve x

$$\%R_x = \%Pass_{x+1} - \%Pass_x \quad (9)$$

**Calculate average particle size, volume, and surface area for each sieve size x for unit mass.**

For the purposes of shape characterization, volume and surface area of an average particle is estimated by using a cubical shape with side dimensions estimated by the average of the retained sieve and next larger sieve dimension.

Average Particle Size: $D_x = \frac{(Sieve_x + Sieve_{x+1})}{2}$ (mm) *(10)*

Average Particle Surface Area (cubical): $PSA_x = 6 * D_x^{\,2}$ ($mm^2$) *(11)*

Average Particle Volume (cubical): $V_x = D_x^{\,3}$ ($mm^3$) *(12)*

**Calculate number of particles per sample unit mass for each sieve size from the size distribution of AASHTO T27 and the respective specific gravities from AASHTO T84 and T85.**

Number of particles per sieve size: $\#P_x = \frac{\%R_x * 1000}{G_{sb} * V_x}$ *(13)*

*Note 2*—A mass of 1 is assumed in *Eq* 13. This calculation determines the weighting factor applied to each sieve size for a material sample, therefore, actual mass is not required.

**Calculate total particle surface area for each sieve size per sample unit mass.**

Particle Surface Area (each sieve x) ($mm^2$): $SSA_x = PSA_x * \#P_x$ *(14)*

**Calculate Sample Surface Area (per unit mass):**

Total Surface Area ($mm^2$): $TSA = \sum_{x=0.075}^{25.0} SSA_x$ *(15)*

Coarse Surface Area ($mm^2$): $CSA = \sum_{x=4.75}^{25.0} SSA_x$ *(16)*

Fine Surface Area ($mm^2$): $FSA = \sum_{x=0.075}^{2.36} SSA_x$ *(17)*

**Calculate Sample Particles Count (per unit mass):**

Total Particles: $$\#TP = \sum_{x=0.075}^{25.0} \#P_x \quad (18)$$

# Coarse Particles: $$\#CP = \sum_{x=4.75}^{25.0} \#P_x \quad (19)$$

# Fine Particles: $$\#FP = \sum_{x=0.075}^{2.36} \#P_x \quad (20)$$

**Calculate Sample Gradient Angularity (weighted by surface area):**

Fine Gradient Angularity: $$FGA = \frac{1}{FSA} \sum_{x=0.075}^{2.36} \left( SA_x * GA_x \right) \quad (21)$$

Coarse Gradient Angularity: $$CGA = \frac{1}{CSA} \sum_{x=4.75}^{25.0} \left( SA_x * GA_x \right) \quad (22)$$

Overall Gradient Angularity: $$GA = \frac{1}{TSA} \sum_{x=0.075}^{25.0} \left( SA_x * GA_x \right) \quad (23)$$

**Calculate Sample Fine Aggregate Form 2D (weighted by surface area):**

$$Form2D = \frac{1}{FSA} \sum_{x=0.075}^{2.36} \left( SA_x * 2D_x \right) \quad (24)$$

**Calculate Sample Coarse Aggregate Texture (weighted by surface area):**

$$TX = \frac{1}{CSA} \sum_{x=4.75}^{25.0} \left( SA_x * TX_x \right) \quad (25)$$

**Calculate Sample Coarse Aggregate Sphericity (weighted by particle count):**

$$SP = \frac{1}{\#CP} \sum_{x=4.75}^{25.0} \left( \#P_x * SP_x \right) \quad (26)$$

**Calculate Sample Sphericity Range Distribution (weighted by particle count):**

% of Particles with Sphericity ≤ 0.3 :

$$SP(0.3) = \frac{1}{\#CP} \sum_{x=4.75}^{25.0} \left( \#P_x * SP(0.3)_x \right) \quad (27)$$

% of Particles with Sphericity 0.3 < SP ≤ 0.7 :

$$SP(0.7) = \frac{1}{\#CP} \sum_{x=4.75}^{25.0} \left[ P_x * SP(0.7)_x \right] \quad (28)$$

% of Particles with Sphericity $0.7 < SP \leq 1.0$ :

$$SP(1.0) = \frac{1}{\#CP} \sum_{x=4.75}^{25.0} \left[ P_x * SP(1.0)_x \right] \quad (29)$$

**Calculate sample weighted percentages of coarse aggregate Flat and Elongated Values (weighted by mass fraction) at the following ratios: ≥1:1, >2:1, >3:1, >4:1, >5:1**

% $d_L/d_S \geq 1$ : $$\%L/S(\geq 1) = \sum_{x=4.75}^{25.0} \left[ \frac{\%R_x * \%L/S(\geq 1)_x}{100} \right] \quad (30)$$

% $d_L/d_S > 2$ : $$\%L/S(> 2) = \sum_{x=4.75}^{25.0} \left[ \frac{\%R_x * \%L/S(> 2)_x}{100} \right] \quad (31)$$

% $d_L/d_S > 3$ : $$\%L/S(> 3) = \sum_{x=4.75}^{25.0} \left[ \frac{\%R_x * \%L/S(> 3)_x}{100} \right] \quad (32)$$

% $d_L/d_S > 4$ : $$\%L/S(> 4) = \sum_{x=4.75}^{25.0} \left[ \frac{\%R_x * \%L/S(> 4)_x}{100} \right] \quad (33)$$

% $d_L/d_S > 5$ : $$\%L/S(> 5) = \sum_{x=4.75}^{25.0} \left[ \frac{\%R_x * \%L/S(> 5)_x}{100} \right] \quad (34)$$

**Calculate the sample weighted percentages of Coarse Aggregate Flat or Elongated (weighted by mass fraction) at the following ratios: ≥1:1, >2:1, >3:1, >4:1, >5:1**

% $d_I/d_S$ or $d_L/d_I \geq 1$ : $$\%ForE(\geq 1) = \sum_{x=4.75}^{25.0} \left[ \frac{\%R_x * \%ForE(\geq 1)_x}{100} \right] \quad (35)$$

% $d_I/d_S$ or $d_L/d_I > 2$ : $$\%ForE(> 2) = \sum_{x=4.75}^{25.0} \left[ \frac{\%R_x * \%ForE(> 2)_x}{100} \right] \quad (36)$$

% $d_I/d_S$ or $d_L/d_I > 3$ : $$\%ForE(> 3) = \sum_{x=4.75}^{25.0} \left[ \frac{\%R_x * \%ForE(> 3)_x}{100} \right] \quad (37)$$

% $d_I/d_S$ or $d_L/d_I > 4$ : $$\%ForE(> 4) = \sum_{x=4.75}^{25.0} \left[ \frac{\%R_x * \%ForE(> 4)_x}{100} \right] \quad (38)$$

% $d_I/d_S$ or $d_L/d_I > 5$ : $$\%ForE(> 5) = \sum_{x=4.75}^{25.0} \left[ \frac{\%R_x * \%ForE(> 5)_x}{100} \right] \quad (39)$$

## CALCULATIONS – MULTIPLE SOURCE BLEND

**Use the calculations in this section to estimate the shape characteristics of multiple material source blends. Each source must be sampled and characterized according to Section 0 calculations.**

### Determine Blend Composition Percentages

$\%AS_n$ = Percent Aggregate Source n

$$\sum_{i=1}^{n} \%AS_i = 100 \qquad (40)$$

where: n = # of aggregate sources

### Calculate Blend Surface Area

Blend Total Surface Area (each sieve):

()

$$SSA_{Blend\_x} = \sum_{i=1}^{n} \sum_{x=0.075}^{37.5} \left[ \frac{\%AS_i * SSA_{ix}}{100} \right]$$

where: x= 0.075 to 25.0 mm

n= # of aggregate sources

Total Surface Area Blend (all sieves x = 0.075 to 25.0 mm)

$$TSA_{Blend} = \sum_{x=0.075}^{25.0} SSA_{Blend\_x} \qquad (41)$$

Coarse Surface Area Blend (sieve x = 4.75 to 25.0):

$$CSA_{Blend} = \sum_{x=4.75}^{25.0} SSA_{Blend\_x} \qquad (42)$$

Fine Surface Area Blend (sieve x =0.075 to 2.36):

$$FSA_{Blend} = \sum_{x=0.075}^{2.36} SSA_{Blend\_x} \qquad (43)$$

### Calculate number of particles per blend unit mass for each sieve size:

$$\#P_{Blend\_x} = \sum_{i=1}^{n} \sum_{x=0.075}^{25.0} \left[ \frac{\%AS_i * \#P_{ix}}{100} \right] \qquad (44)$$

### Calculate number of particles per blend unit mass

Total Particle Count Blend:

$$\#TP_{Blend} = \sum_{x=0.075}^{25.0} \#P_{Blend\_x} \qquad (45)$$

# Coarse Particles Blend:

$$\#CP_{Blend} = \sum_{x=4.75}^{25.0} \#P_{Blend\_x} \quad (46)$$

# Fine Particles Blend:

$$\#FP_{Blend} = \sum_{x=0.075}^{2.36} \#P_{Blend\_x} \quad (47)$$

**Calculate Blend Gradient Angularity for each size x = 0.075 to 25.0 mm and combined (weighted by surface area):**

$$GA_{Blend\_x} = \frac{1}{SSA_{Blend\_x}} \left[ \sum_{i=1}^{i} \left[ \frac{\%AS_i * SSA_{ix} * GA_{ix}}{100} \right] \right] \quad (48)$$

Blend Fine Gradient Angularity:

$$FGA_{Blend} = \frac{1}{FSA_{Blend}} \left[ \sum_{x=0.075}^{2.36} SSA_{Blend\_x} * GA_{Blend\_x} \right] \quad (49$$

Blend Coarse Gradient Angularity:

$$CGA_{Blend} = \frac{1}{CSA_{Blend}} \left[ \sum_{x=4.75}^{25.0} SSA_{Blend\_x} * GA_{Blend\_x} \right] \quad (50)$$

Blend Overall Gradient Angularity:

$$GA_{Blend} = \frac{1}{TSA_{Blend}} \left[ \sum_{x=0.075}^{25.0} SSA_{Blend\_x} * GA_{Blend\_x} \right] \quad (51)$$

**Calculate Blend Fine Aggregate Form 2D for each size x = 0.075 to 2.36 mm and combined (weighted by surface area):**

$$Form2D_{Blend\_x} = \frac{1}{SSA_{Blend\_x}} \left[ \sum_{i=1}^{n} \left[ \frac{\%AS_i * SSA_{ix} * 2D_{ix}}{100} \right] \right] \quad (52)$$

Blend Form 2D:

$$Form2D_{Blend} = \frac{1}{FSA_{Blend}} \left[ \sum_{x=0.075}^{2.36} SSA_{Blend\_x} * 2D_{Blend\_x} \right] \quad (53)$$

**Calculate Blend Texture for each size x = 4.75 to 25.0 mm and combined (weighted by coarse aggregate surface area):**

$$TX_{Blend\_x} = \frac{1}{SSA_{Blend\_x}} \left[ \sum_{i=1}^{n} \left[ \frac{\%AS_i * SSA_{ix} * TX_{ix}}{100} \right] \right] \quad (54)$$

Blend Texture:

$$TX_{Blend} = \frac{1}{CSA_{Blend}}\left[\sum_{x=4.75}^{25.0} CSA_{Blend\_x} * TX_{Blend\_x}\right] \quad (55)$$

**Calculate Average Blend Sphericity for each size 4.75 to 25.0 and blend (weighted by coarse particle count):**

$$SP_{Blend\_x} = \frac{1}{\#P_{Blend\_x}}\left[\sum_{i=1}^{n}\left[\frac{\%AS_i * \#P_{ix} * SP_{ix}}{100}\right]\right] \quad (56)$$

Blend Sphericity:

$$SP_{Blend} = \frac{1}{\#CP_{Blend}}\left[\sum_{x=4.75}^{25.0} \#P_{Blend\_x} * SP_{Blend\_x}\right] \quad (57)$$

**Calculate Blend Sphericity Distribution for each sieve 4.75 to 25.0 mm and blend (weighted by coarse particle count):**

% of Particles with Sphericity ≤ 0.3 (Blend):

$$SP(0.3)_{Blend\_x} = \frac{1}{\#P_{Blend\_x}}\left[\sum_{i=1}^{n}\left[\frac{\%AS_i * \#P_{ix} * SP(0.3)_{ix}}{100}\right]\right] \quad (58)$$

$$SP(0.3)_{Blend} = \frac{1}{\#CP_{Blend}}\left[\sum_{x=4.75}^{25.0} \#P_{Blend\_x} * SP(0.3)_{Blend\_x}\right] \quad (59)$$

% of Particles with Sphericity 0.3 < SP ≤ 0.7 (Blend):

$$SP(0.7)_{Blend\_x} = \frac{1}{\#P_{Blend\_x}}\left[\sum_{i=1}^{n}\left[\frac{\%AS_i * \#P_{ix} * SP(0.7)_{ix}}{100}\right]\right] \quad (60)$$

$$SP(0.7)_{Blend} = \frac{1}{\#CP_{Blend}}\left[\sum_{x=4.75}^{25.0} \#P_{Blend\_x} * SP(0.7)_{Blend\_x}\right] \quad (61)$$

% of Particles with Sphericity 0.7 < SP ≤ 1.0 (Blend):

$$SP(1.0)_{Blend\_x} = \frac{1}{\#P_{Blend\_x}}\left[\sum_{i=1}^{n}\left[\frac{\%AS_i * \#P_{ix} * SP(1.0)_{ix}}{100}\right]\right] \quad (62)$$

$$SP(1.0)_{Blend} = \frac{1}{\#CP_{Blend}}\left[\sum_{x=4.75}^{25.0} \#P_{Blend\_x} * SP(1.0)_{Blend\_x}\right] \quad (63)$$

**Calculate combined Flat <u>and</u> Elongated Values for each sieve 4.75 to 25.0 mm and blend (weighted by mass fraction):**

% $d_L/d_S \geq 1$ (Blend):

$$\%L/S(\geq 1)_{Blend\_x} = \left[\sum_{i=1}^{n}\left[\frac{\%AS_i * \%R_{ix} * \%L/S(\geq 1)_{ix}}{100^2}\right]\right] \quad (64)$$

$$\%L/S(\geq 1)_{Blend} = \left[\sum_{x=4.75}^{25.0}\%L/S(\geq 1)_{Blend\_x}\right] \quad (65)$$

% $d_L/d_S > 2$ (Blend):

$$\%L/S(>2)_{Blend\_x} = \left[\sum_{i=1}^{n}\left[\frac{\%AS_i * \%R_{ix} * \%L/S(>2)_{ix}}{100^2}\right]\right] \quad (66)$$

$$\%L/S(>2)_{Blend} = \left[\sum_{x=4.75}^{25.0}\%L/S(>2)_{Blend\_x}\right] \quad (67)$$

% $d_L/d_S > 3$ (Blend):

$$\%L/S(>3)_{Blend\_x} = \left[\sum_{i=1}^{n}\left[\frac{\%AS_i * \%R_{ix} * \%L/S(>3)_{ix}}{100^2}\right]\right] \quad (68)$$

$$\%L/S(>3)_{Blend} = \left[\sum_{x=4.75}^{25.0}\%L/S(>3)_{Blend\_x}\right] \quad (69)$$

% $d_L/d_S > 4$ (Blend):

$$\%L/S(>4)_{Blend\_x} = \left[\sum_{i=1}^{n}\left[\frac{\%AS_i * \%R_{ix} * \%L/S(>4)_{ix}}{100^2}\right]\right] \quad (70)$$

$$\%L/S(>4)_{Blend} = \left[\sum_{x=4.75}^{25.0}\%L/S(>4)_{Blend\_x}\right] \quad (71)$$

% $d_L/d_S \leq 5$ (Blend):

$$\%L/S(>5)_{Blend\_x} = \left[\sum_{i=1}^{n}\left[\frac{\%AS_i * \%R_{ix} * \%L/S(>5)_{ix}}{100^2}\right]\right] \quad (72)$$

$$\%L/S(>5)_{Blend} = \left[\sum_{x=4.75}^{37.5}\%L/S(>5)_{Blend\_x}\right] \quad (73)$$

**Calculate Flat <u>or</u> Elongated Values for each sieve 4.75 to 25.0 mm and blend (weighted by mass fraction):**

% $d_I/d_S$ or $d_L/d_I \geq 1$ : (Blend):

$$\%ForE(\geq 1)_{Blend\_x} = \left[\sum_{i=1}^{n}\left[\frac{\%AS_i * \%R_{ix} * \%ForE(\geq 1)_{ix}}{100^2}\right]\right] \quad (74)$$

$$\%ForE(\geq 1)_{Blend} = \left[\sum_{x=4.75}^{25.0}\left(\%ForE(\geq 1)_{Blend\_x}\right)\right] \quad (75)$$

% $d_I/d_S$ or $d_L/d_I > 2$ : (Blend):

$$\%ForE(> 2)_{Blend\_x} = \left[\sum_{i=1}^{n}\left[\frac{\%AS_i * \%R_{ix} * \%ForE(> 2)_{ix}}{100^2}\right]\right] \quad (76)$$

$$\%ForE(> 2)_{Blend} = \left[\sum_{x=4.75}^{25.0}\left(\%ForE(> 2)_{Blend\_x}\right)\right] \quad (77)$$

% $d_I/d_S$ or $d_L/d_I > 3$ : (Blend):

$$\%ForE(> 3)_{Blend\_x} = \left[\sum_{i=1}^{n}\left[\frac{\%AS_i * \%R_{ix} * \%ForE(> 3)_{ix}}{100^2}\right]\right] \quad (78)$$

$$\%ForE(> 3)_{Blend} = \left[\sum_{x=4.75}^{25.0}\left(\%ForE(> 3)_{Blend\_x}\right)\right] \quad (79)$$

% $d_I/d_S$ or $d_L/d_I > 4$ : (Blend):

$$\%ForE(> 4)_{Blend\_x} = \left[\sum_{i=1}^{i}\left[\frac{\%AS_i * \%R_{ix} * \%ForE(> 4)_{ix}}{100^2}\right]\right] \quad (80)$$

$$\%ForE(> 4)_{Blend} = \left[\sum_{x=4.75}^{25.0}\left(\%ForE(> 4)_{Blend\_x}\right)\right] \quad (81)$$

% $d_I/d_S$ or $d_L/d_I > 5$ : (Blend):

$$\%ForE(> 5)_{Blend\_x} = \left[\sum_{i=1}^{n}\left[\frac{\%AS_i * \%R_{ix} * \%ForE(> 5)_{ix}}{100^2}\right]\right] \quad (82)$$

$$\%ForE(> 5)_{Blend} = \left[\sum_{x=4.75}^{25.0}\left(\%ForE(> 5)_{Blend\_x}\right)\right] \quad (83)$$

## REPORT

**Report the following information:**

A sample report format is presented in Appendix X1

**Project name**

**Date of the analysis**

**Material sample identifications: type, source, size, gradation.**

**Number of particles analyzed for each size.**

**Material shape property mean and standard deviation. Graphical representations of the property distributions may be included.**

---

## PRECISION AND BIAS

***Precision*—This practice uses data generated from other testing methods to develop cumulative information, therefore the precision of the values generated in this practice are established by the precision of the standards used to collect the raw data.**

***Bias*—Since there is no accepted reference device suitable for determining the bias in this method, no statement of bias is made.**

---

## KEYWORDS

**aggregate; angularity; consensus property, shape, texture, form, elongation**

# Appendix X1: Sample Report

## Stockpile Information

| | |
|---|---|
| Date: | 2/5/09 |
| Project: | 41_Granite_1 |
| Technician: | mjg |
| Workbook Name: | 41_Granite1_AIMS_Stockpile_v3.6.xlsm |
| Description: | |

| | Include | Estimate | Nominal Sieve Size | ◉ % Passing | ○ % Retained |
|---|---|---|---|---|---|
| | | ☐ | 37.5 (1.5") | 100.0% | 0.0% |
| Coarse | ☑ | ☐ | 25.0 (1.0") | 93.0% | 7.0% |
| | ☑ | ☐ | 19.0 (3/4") | 85.0% | 8.0% |
| | ☑ | ☐ | 12.5 (1/2") | 70.0% | 15.0% |
| | ☑ | ☐ | 9.5 (3/8") | 55.0% | 15.0% |
| | ☑ | ☐ | 4.75 (#4) | 35.0% | 20.0% |
| Fine | ☑ | ☐ | 2.36 (#8) | 25.0% | 10.0% |
| | ☑ | ☐ | 1.18 (#16) | 15.0% | 10.0% |
| | ☑ | ☐ | 0.60 (#30) | 10.0% | 5.0% |
| | ☑ | ☐ | 0.30 (#50) | 5.0% | 5.0% |
| | ☑ | ☐ | 0.15 (#100) | 0.0% | 5.0% |
| | ☑ | ☐ | 0.075 (#200) | 0.0% | 0.0% |
| | | | Passing #200 | 0.0% | 0.0% |

| | |
|---|---|
| Gsb(Coarse)= | 2.500 |
| Gsb (Fine)= | 2.500 |

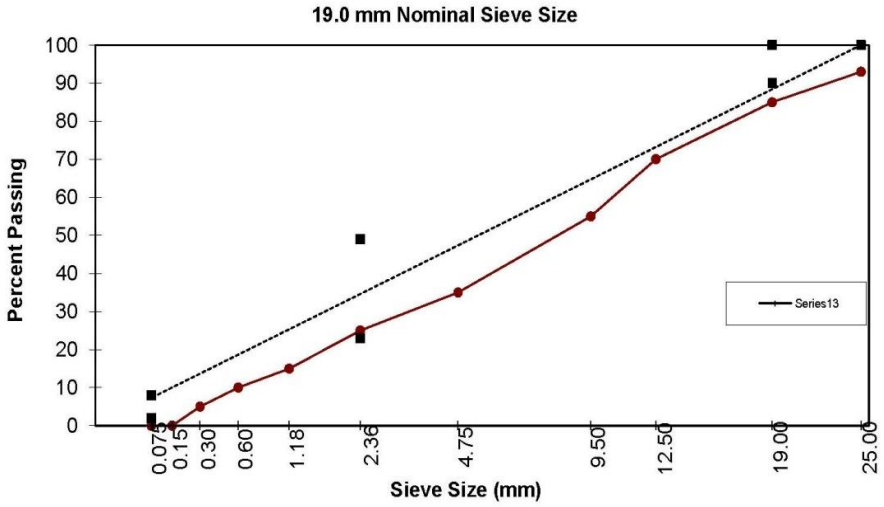

## AIMS Stockpile Summary

| | | | |
|---|---|---|---|
| Project Name: | 41_Granite_1 | Date: | 2/5/09 |
| Workbook: | 41_Granite1_AIMS_Stockpile_v3.6.xlsm | Technician: | mjg |
| Description: | | | |

### Combined Properties (weighted)

| | | | | | | | |
|---|---|---|---|---|---|---|---|
| 2D Form (Fine) | 7.95 | Sphericity (Coarse) | % | Flat & Elongated Ratio (Coarse) | % | Flat or Elongated Ratio (Coarse) | Cum.% |
| Angularity (Coarse & Fine) | 3457.5 | Low ( ≤ 0.3) | 0.0% | L/S ≥ 1:1 | 65.0% | F or E ≥ 1:1 | 65.0% |
| Fine Angularity | 3501.3 | Medium ( 0.3 - 0.7) | 44.3% | L/S > 2:1 | 48.0% | F or E > 1:2 | 25.7% |
| Coarse Angularity | 3039.7 | High ( 0.7 - 1.0) | 20.7% | L/S > 3:1 | 23.3% | F or E > 1:3 | 4.8% |
| | | | | L/S > 4:1 | 7.3% | F or E > 1:4 | 0.8% |
| Texture (Coarse) | 387.6 | Sphericity (Coarse) | 0.67 | L/S > 5:1 | 2.0% | F or E > 1:5 | 0.8% |

### Form2D

| Size | Particles in Range | Average | Standard Deviation | Low ( ≤ 6 ) # | Low ( ≤ 6 ) % | ( ≤ 6 ) Cum. % | Medium ( 6 - 12 ) # | Medium ( 6 - 12 ) % | ( ≤ 12 ) Cum. % | High ( 12 - 20 ) # | High ( 12 - 20 ) % | ( ≤ 20 ) Cum. % | Out of Range # |
|---|---|---|---|---|---|---|---|---|---|---|---|---|---|
| 2.36 (#8) | 151 | 7.7 | 1.9 | 33 | 21.9% | 21.9% | 113 | 74.8% | 96.7% | 5 | 3.3% | 100.0% | 0 |
| 1.18 (#16) | 150 | 7.5 | 1.8 | 32 | 21.3% | 21.3% | 116 | 77.3% | 98.7% | 2 | 1.3% | 100.0% | 0 |
| 0.60 (#30) | 150 | 8.0 | 2.1 | 26 | 17.3% | 17.3% | 119 | 79.3% | 96.7% | 5 | 3.3% | 100.0% | 0 |
| 0.30 (#50) | 151 | 8.0 | 2.2 | 28 | 18.5% | 18.5% | 115 | 76.2% | 94.7% | 8 | 5.3% | 100.0% | 0 |
| 0.15 (#100) | 151 | 8.1 | 2.0 | 17 | 11.3% | 11.3% | 128 | 84.8% | 96.0% | 6 | 4.0% | 100.0% | 0 |
| 0.075 (#200) | 146 | 8.9 | 2.8 | 19 | 13.0% | 13.0% | 104 | 71.2% | 84.2% | 23 | 15.8% | 100.0% | 5 |

### Angularity

| Size | Particles in Range | Average | Standard Deviation | Low ( ≤ 3300 ) # | Low ( ≤ 3300 ) % | (≤ 3300) Cum. % | Medium(3300-6600) # | Medium(3300-6600) % | (≤ 6600) Cum. % | High(6600-10000) # | High(6600-10000) % | (≤ 10000) Cum. % | Out of Range # |
|---|---|---|---|---|---|---|---|---|---|---|---|---|---|
| 37.5 (1.5") | | | | | | | | | | | | | |
| 25.0 (1.0") | 50 | 2873.0 | 493.1 | 37 | 74.0% | 74.0% | 13 | 26.0% | 100.0% | 0 | 0.0% | 100.0% | 0 |
| 19.0 (3/4") | 50 | 2841.5 | 639.0 | 41 | 82.0% | 82.0% | 9 | 18.0% | 100.0% | 0 | 0.0% | 100.0% | 0 |
| 12.5 (1/2") | 50 | 3138.7 | 597.3 | 28 | 56.0% | 56.0% | 22 | 44.0% | 100.0% | 0 | 0.0% | 100.0% | 0 |
| 9.5 (3/8") | 50 | 3251.6 | 694.5 | 27 | 54.0% | 54.0% | 23 | 46.0% | 100.0% | 0 | 0.0% | 100.0% | 0 |
| 4.75 (#4) | 50 | 2963.7 | 590.8 | 37 | 74.0% | 74.0% | 13 | 26.0% | 100.0% | 0 | 0.0% | 100.0% | 0 |
| 2.36 (#8) | 151 | 3454.8 | 918.6 | 71 | 47.0% | 47.0% | 79 | 52.3% | 99.3% | 1 | 0.7% | 100.0% | 0 |
| 1.18 (#16) | 150 | 3288.5 | 802.0 | 81 | 54.0% | 54.0% | 69 | 46.0% | 100.0% | 0 | 0.0% | 100.0% | 0 |
| 0.60 (#30) | 150 | 3642.0 | 949.7 | 58 | 38.7% | 38.7% | 90 | 60.0% | 98.7% | 2 | 1.3% | 100.0% | 0 |
| 0.30 (#50) | 151 | 3650.0 | 984.1 | 62 | 41.1% | 41.1% | 89 | 58.9% | 100.0% | 0 | 0.0% | 100.0% | 0 |
| 0.150 (#100) | 151 | 3451.5 | 1060.6 | 83 | 55.0% | 55.0% | 66 | 43.7% | 98.7% | 2 | 1.3% | 100.0% | 0 |
| 0.075 (#200) | 151 | 2595.7 | 1241.4 | 126 | 83.4% | 83.4% | 24 | 15.9% | 99.3% | 1 | 0.7% | 100.0% | 0 |

## AIMS Stockpile Summary

| | | | |
|---|---|---|---|
| Project Name: | 41_Granite_1 | Date: | 2/5/09 |
| Workbook: | 41_Granite1_AIMS_Stockpile_v3.6.xlsm | Technician: | mjg |
| Description: | | | |

### Texture

| Size | Particles in Range | Average | Standard Deviation | Low ( ≤ 260) # | Low ( ≤ 260) % | (≤ 260) Cum. % | Medium (260 - 550) # | Medium (260 - 550) % | (≤ 550) Cum. % | High ( 550 - 1000 ) # | High ( 550 - 1000 ) % | (≤ 1000) Cum. % | Out of Range # |
|---|---|---|---|---|---|---|---|---|---|---|---|---|---|
| 37.5 (1.5") | | | | | | | | | | | | | |
| 25.0 (1.0") | 50 | 461.0 | 84.8 | 0 | 0.0% | 0.0% | 45 | 90.0% | 90.0% | 5 | 10.0% | 100.0% | 0 |
| 19.0 (3/4") | 50 | 480.4 | 90.5 | 1 | 2.0% | 2.0% | 39 | 78.0% | 80.0% | 10 | 20.0% | 100.0% | 0 |
| 12.5 (1/2") | 50 | 455.5 | 119.8 | 1 | 2.0% | 2.0% | 41 | 82.0% | 84.0% | 8 | 16.0% | 100.0% | 0 |
| 9.5 (3/8") | 50 | 430.5 | 128.8 | 5 | 10.0% | 10.0% | 38 | 76.0% | 86.0% | 7 | 14.0% | 100.0% | 0 |
| 4.75 (#4) | 50 | 342.5 | 135.2 | 13 | 26.0% | 26.0% | 33 | 66.0% | 92.0% | 4 | 8.0% | 100.0% | 0 |

### Sphericity

| Size | Particles in Range | Average | Standard Deviation | Low ( ≤ 0.3) # | Low ( ≤ 0.3) % | (≤ 0.3) Cum. % | Medium ( 0.3 - 0.7) # | Medium ( 0.3 - 0.7) % | (≤ 0.7) Cum. % | High ( 0.7 - 1.0) # | High ( 0.7 - 1.0) % | (≤ 1.0) Cum. % | Out of Range # |
|---|---|---|---|---|---|---|---|---|---|---|---|---|---|
| 37.5 (1.5") | | | | | | | | | | | | | |
| 25.0 (1.0") | 49 | 0.68 | 0.08 | 0 | 0.0% | 0.0% | 30 | 61.2% | 61.2% | 19 | 38.8% | 100.0% | 1 |
| 19.0 (3/4") | 49 | 0.62 | 0.09 | 0 | 0.0% | 0.0% | 39 | 79.6% | 79.6% | 10 | 20.4% | 100.0% | 1 |
| 12.5 (1/2") | 49 | 0.62 | 0.09 | 0 | 0.0% | 0.0% | 37 | 75.5% | 75.5% | 12 | 24.5% | 100.0% | 1 |
| 9.5 (3/8") | 50 | 0.61 | 0.10 | 0 | 0.0% | 0.0% | 37 | 74.0% | 74.0% | 13 | 26.0% | 100.0% | 0 |
| 4.75 (#4) | 50 | 0.67 | 0.12 | 0 | 0.0% | 0.0% | 28 | 56.0% | 56.0% | 22 | 44.0% | 100.0% | 0 |

### Flat and Elongated Distribution

| Size | Particles in Range | L/S ≥ 1:1 # | L/S ≥ 1:1 % | L/S > 2:1 # | L/S > 2:1 % | L/S > 3:1 # | L/S > 3:1 % | L/S > 4:1 # | L/S > 4:1 % | L/S > 5:1 # | L/S > 5:1 % | Out of Range # |
|---|---|---|---|---|---|---|---|---|---|---|---|---|
| 37.5 (1.5") | | | | | | | | | | | | |
| 25.0 (1.0") | 49 | 49 | 100.0% | 33 | 67.3% | 9 | 18.4% | 1 | 2.0% | 0 | 0.0% | 1 |
| 19.0 (3/4") | 49 | 49 | 100.0% | 42 | 85.7% | 20 | 40.8% | 5 | 10.2% | 1 | 2.0% | 1 |
| 12.5 (1/2") | 49 | 49 | 100.0% | 43 | 87.8% | 21 | 42.9% | 6 | 12.2% | 1 | 2.0% | 1 |
| 9.5 (3/8") | 50 | 50 | 100.0% | 39 | 78.0% | 25 | 50.0% | 7 | 14.0% | 1 | 2.0% | 0 |
| 4.75 (#4) | 50 | 50 | 100.0% | 29 | 58.0% | 12 | 24.0% | 6 | 12.0% | 3 | 6.0% | 0 |

### Flat or Elongated Distribution

| Size | Particles in Range | F or E ≥ 1:1 # | F or E ≥ 1:1 % | F or E >2:1 # | F or E >2:1 % | F or E >3:1 # | F or E >3:1 % | F or E >4:1 # | F or E >4:1 % | F or E >5:1 # | F or E >5:1 % | Out of Range # |
|---|---|---|---|---|---|---|---|---|---|---|---|---|
| 37.5 (1.5") | | | | | | | | | | | | |
| 25.0 (1.0") | 49 | 49 | 100.0% | 12 | 24.5% | 2 | 4.1% | 0 | 0.0% | 0 | 0.0% | 1 |
| 19.0 (3/4") | 49 | 49 | 100.0% | 23 | 46.9% | 4 | 8.2% | 0 | 0.0% | 0 | 0.0% | 1 |
| 12.5 (1/2") | 49 | 49 | 100.0% | 23 | 46.9% | 4 | 8.2% | 0 | 0.0% | 0 | 0.0% | 1 |
| 9.5 (3/8") | 50 | 50 | 100.0% | 24 | 48.0% | 2 | 4.0% | 0 | 0.0% | 0 | 0.0% | 0 |
| 4.75 (#4) | 50 | 50 | 100.0% | 15 | 30.0% | 5 | 10.0% | 2 | 4.0% | 2 | 4.0% | 0 |

**AIMS Angularity**

| | | | |
|---|---|---|---|
| Project Name: | 41_Granite_1 | Date: | 2/5/09 |
| Workbook: | 41_Granite1_AIMS_Stockpile_v3.6.xlsm | Technician: | mjg |
| Description: | | | |

| | | | | | | | | |
|---|---|---|---|---|---|---|---|---|
| | | | # | % | | Cum. % | | # | % |
| Particles in Range | 1154 | Low ( ≤ 3300) | 651 | 56.4% | ( ≤ 3300 ) | 56.4% | -σ < n < σ | 814 | 70.5% |
| Average | 3274.7 | Medium ( 3300 - 6600 ) | 497 | 43.1% | ( ≤ 6600 ) | 99.5% | -2σ < n < 2σ | 1105 | 95.8% |
| Std. Deviation | 995.6 | High ( 6600 - 10000 ) | 6 | 0.5% | ( ≤ 10000 ) | 100.0% | -3σ < n < 3σ | 1144 | 99.1% |
| Median | 3170.6 | Out of Range | 0 | | | | n<-3σ or n>3σ | 10 | 0.9% |
| Mode | 3330.1 | | | | | | | | |

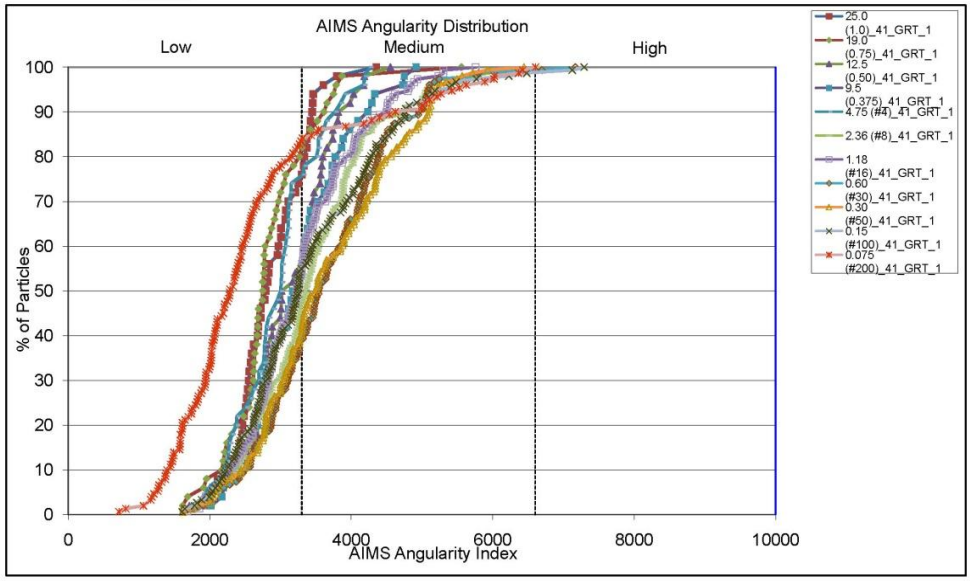

# VITA

Andrew James Muras received his Bachelor of Science degree in civil engineering from Texas A&M University in December 2007. He entered graduate school at Texas A&M University in January 2008 and received his Master of Science degree in May 2010. While working towards his master's degree, he worked as a research assistant at Texas Transportation Institute (TTI) in College Station, Texas.

He can be reached at the email address andrewmuras03@yahoo.com, or at the mailing address shown below.

Texas Transportation Institute
CE/TTI Building Floor 5
Texas A&M university System
College Station, TX 77843-3135